NASA Contractor Report 189727

Phased Array Feed Design Technology for Large Aperture Microwave Radiometer (LAMR) Earth Observations

H. K. Schuman
ARC Professional Services Group
Rome, New York

Research Triangle Institute
Research Triangle Park, North Carolina

Contract NAS1-18925
December 1992

National Aeronautics and Space Administration

Langley Research Center
Hampton, Virginia 23665-5225

ABSTRACT

An assessment of the potential and limitations of phased array antennas in space based geophysical precision radiometry is described. Mathematical models exhibiting the dependence of system and scene temperatures and system sensitivity on phased array antenna parameters and components such as phase shifters and low noise amplifiers (LNAs) are developed. Emphasis is given to minimum noise temperature designs wherein the LNA's are located at the array level, one per element or subarray. Two types of combiners are considered: array lenses (space feeds) and corporate networks. The result of a survey of suitable components and devices is described. The data obtained from that survey is used in conjunction with the mathematical models to yield an assessment of effective array antenna noise temperature for representative geostationary and low earth orbit systems. Practical methods of calibrating a space based phased array radiometer are briefly addressed as well. An interesting finding is that, with amplifiers located at the element level of an N element array, amplifier phase fluctuations have negligible impact on sensitivity and that amplifier gain fluctuations that are uncorrelated between amplifiers have $N^{1/2}$ times less detrimental impact on sensitivity than do fully correlated gain fluctuations. Also, for space based systems, array lens combiners are apt to exhibit lower noise temperatures than corporate network combiners due primarily to the negligible insertion loss associated with lens combiners.

TABLE OF CONTENTS

APPENDICES

SECTION 1

INTRODUCTION AND SUMMARY

This report contains findings and system modeling associated with an effort to assess the potential and limitations of phased array antenna microwave/mmW precision radiometry and to identify perhaps novel designs for achieving satisfactory performance with acceptable complexity and weight. The intended function of the radiometer would be space based geophysical sensing. Principal architectures under consideration for this effort included:

- o RF amplifiers (LNAs) located at the "array level," each associated with an unique phase shifter,
- o space feed "lens" and corporate network constrained feed combiners, and
- o array fed reflectors as well as stand alone arrays.

Reasonably detailed expressions for models of array lens and corporate network combiner gains have been developed as described in Appendices A and B. These models were used in the development of system models, as described in Section 2 and 3 and Appendix C for use in quantitatively assessing the impact of component limitations on sensitivity (minimum detectable signal) and accuracy (absolute temperature), and conversely, the limitations of components necessary to achieve specified sensitivities and accuracies. Components under consideration included LNAs, phase shifters, radiating elements, and combiners. The results of a survey of state of the art performance of such components is described in Section 5.

Specific items that were addressed in this effort are described in sub-sections 1.1, 1.2, and 1.3 to follow. Other items requiring attention, but which could not be dealt with satisfactorily during this effort, are outlined in subsection 1.4.

1.1 Sensitivity

Sensitivity refers to the minimum detectable signal of the radiometer system. Sensitivity is limited in part by the random fluctuations of noise. As discussed in Section 3, for a square law detection receiver, the minimum detectable change in "equivalent" receiver input noise temperature, ΔT, is directly proportional to the average "equivalent" receiver input noise temperature, T, and inversely proportional to the square root of the product of predetection bandwidth, B, and dwell time, τ. Thus, for a given bandwidth, the larger the average temperature, the longer the dwell time required to achieve a desired sensitivity. It is imperative, therefore, to limit T however possible. Because phased array antennas usually are inherently lossy, especially if digital phase shifters are employed, it is likely to be necessary to precede the phase shifters with low noise amplifiers (LNAs) if T is to be confined to a manageable level. The relations presented in Sections 2 and 3 and Appendices A and B can be used to quantitatively assess the impact of number of array elements, N; phase shifter loss; amplifier noise figure and gain; and combiner loss, mismatch, and type on T, and, in turn, on ΔT, τ, and B. A preliminary analysis of representative geostationary and low earth orbit systems (Section 6) suggests that the effective noise temperature contributed by the active array with 20 dB gain LNAs can be limited to under 700 K in either system.

Sensitivity is also affected by short term (seconds or less) fluctuations in amplifier performance. Total power radiometers are particularly sensitive to this effect, and since total power radiometers are considerably less complex than Dicke radiometers, it is important that this effect be suitably assessed. Such an assessment can be carried out via the relations developed in Section 3 and Appendix C. From the derivations therein, it is evident that amplifier phase

fluctuations have negligible impact on sensitivity* and that amplifier gain fluctuations that are uncorrelated between amplifiers in the array have $N^{1/2}$ times less detrimental impact on sensitivity than do correlated gain fluctuations. (See also Issue 1 in subsection 1.4.)

1.2 Combiner

A space fed array (lens) combiner has less dissipative losses than does a corporate network constrained feed. Also, the lens is likely to be of lighter weight. The corporate combiner, on the other hand, permits better impedance match control, on the feed side. Active impedance mismatch experienced by the feed side radiating elements of the lens was included in the lens model (Section 2 and Appendix A). A quantitative comparison between both types of combiners was performed (Section 6). For space based systems, array lens combiners are apt to exhibit lower noise temperatures.

1.3 Calibration

Methods of calibrating an active phased array antenna radiometer were addressed only briefly (Section 4). Because impedance mismatch varies with beam position - and phase shifter loss, in general, varies with beam position as well - a separate calibration measurement for each beam position would appear to be necessary. Some form of "relative calibration," however, may prove a satisfactory alternative. Consequently, a study is suggested to determine the existence of relations between beam position that may be obtained via a one time measurement

*This conclusion has been verified, recently, as part of a study conducted by Grumman Aerospace Corporation [1]. The analysis presented here was extended at Grumman to quantify the second order effects arising from amplifier phase fluctuations.

and such that these relations can be used, in turn, to calibrate all beam positions from calibration measurements taken regularly at one, or only a few, beam positions. The feasibility of constructing a sufficiently large yet well controlled calibration source and of electronically focusing the array onto such source, thus avoiding the need for physical motion, must be addressed as well.

An alternative, novel method that permits rapid, frequent calibration of all beam positions directly also is described in Section 4. In this method, the array aperture is covered with a temperature controlled linearly polarized screen and polarization switching at the element level allows alternate measurements of scene temperature and screen temperature. Such a method is particularly attractive if a Dicke type radiometer is required. However, the method would require that the scene temperature measurements be limited to single polarization.

1.4 Other Issues

Other concerns must be addressed as part of a comprehensive study aimed at designing a suitable phased array antenna radiometer for space based geophysical sensing. These concerns are described below. They were not addressed to any significant extent during the effort described here.

1. Levels and causes of rapid fluctuations in LNA performance (see subsection 1.1). An appropriate study, in conjunction with pertinent experiments, would be highly desirable because of the probable absence of sufficient data. (Perhaps bench tests envisioned at NASA/Langley could address this issue.) Recent past technology had been such that RF amplifier gain variations on the order of 10^{-3} or 10^{-4} were achievable but only with difficult proper control of power supply and environment temperature [2]. Since 1 K resolution is roughly commensurate with 10^{-4} gain fluctuations, it

is imperative that the amount of supply and temperature control of potential devices be carefully assessed as well as methods of achieving adequate control. If adequate control is not feasible, the more complex Dicke type radiometer would be mandatory. There is evidence that distributed amplification enhances stability (subsection 1.1, Section 3, and Appendix C) but only if the amplifier fluctuations are reasonably uncorrelated. The nature of the fluctuations, therefore, must be assessed as well.

2. Calibration Experiment. The potential accuracy of the "relative calibration" procedure described in subsection 1.3 and Section 4 must be assessed via an appropriate experiment. The Air Force's Rome Laboratory has a 104 element solid state planar array with an LNA and fully controllable four-bit phase shifter associated with each element. This array would be an excellent candidate with which to conduct such an experiment. Suitable measurement facilities are available at Rome Laboratory, as well as calibration temperature sources.

3. Temperature dependence of phase shifter loss. Such a study may prove essential to achieving high accuracy. Finite phase shifter loss, for example, in the phased array microwave radiometer on board Nimbus spacecrafts require calibration as part of the effort to achieve the stated 2 K absolute accuracy [3]. It was found that the temperature dependent and scan dependent losses associated with the phase shifters were separable, a condition that greatly simplified development of calibration relations. Digital phase shifter loss, although typically larger than that for ferrite phase shifters, may be less temperature dependent.

4. Multiband array design. The design of a multiband, dual polarization array would be essential to the realization of a suitable broadband system because of the substantial frequency dependence of phased arrays, and of phase shifters and amplifiers. The array bandwidth limitations of the radiating element described in Section 5.2 would require three overlapping (shared aperture) arrays to cover the minimum bandwidth (19 GHz - 60 GHz) recommended in the recently completed "Science Benefits" study [4].

5. Impact of failed elements (LNAs and/or phase shifters). The impact is expected to be one of "graceful degradation," but a quantitative assessment of the impact on sensitivity and calibration is needed.

6. Methods of achieving large field of view while retaining high beam efficiency. The larger the field of view and the greater the spatial resolution, the greater the number of array elements required (subsection 5.1). If a large reflector is included in the antenna system to trade field of view for spatial resolution, the array fed reflector architecture would require considerable study if a reasonable field of view is to be retained. A principal limitation would be the degradation of beam efficiency arising from optical aberration with scan, and high beam efficiency is required to minimize the impact of sidelobe energy on calibration error. The degradation is especially pronounced in offset feed designs.

7. Calibration of array fed reflectors. Because the reflector may not entirely intercept the bulk of the radiated near field of the array antenna for each beam position, and because of varying temperatures throughout the reflector surface, the noise resulting from reflector

losses may vary between beam positions, perhaps causing substantial absolute temperature measurement errors. A study of the severity of this effect is warranted.

SECTION 2

NOISE TEMPERATURE

The essential features of two types of phased array receiving antennas are shown in Figures 2-1 and 2-2. They differ only in the "combiner" section. One employs a space feed "lens" combiner and the other a constrained feed "corporate" combiner. The array antenna could be "stand alone" or could function as the feed of a multireflector system.

The noise temperature referred to the receiver input, T, can be expressed as the sum of four terms:

$$T = T_{ary} + T_{sig} + T_{ref} + T_{rn} \qquad (2\text{-}1)$$

where

T_{ary} = phased array antenna induced (uncorrelated) noise temperature

T_{sig} = signal (scene) induced noise temperature

T_{ref} = reflector/radome induced noise temperature

T_{rn} = receiver generated (equivalent input) noise temperature

Expressions for T_{ary}, T_{sig}, and T_{ref} are presented in the subsections to follow.

2.1 Phased Array Antenna Induced (Uncorrelated) Noise Temperature

There are three contributions to the phased array induced noise temperature at the receiver input, that from the low noise amplifier (T_{LNA}), phase shifter (T_{ϕ}), and combiner (T_c). Expressions for these temperatures are

$$T_{LNA} = 290\ (F_a - 1)\ \frac{GG_u}{N}$$

$$T_{\phi} = T_o \left(1 - \frac{1}{L_{\phi}}\right) G_u$$

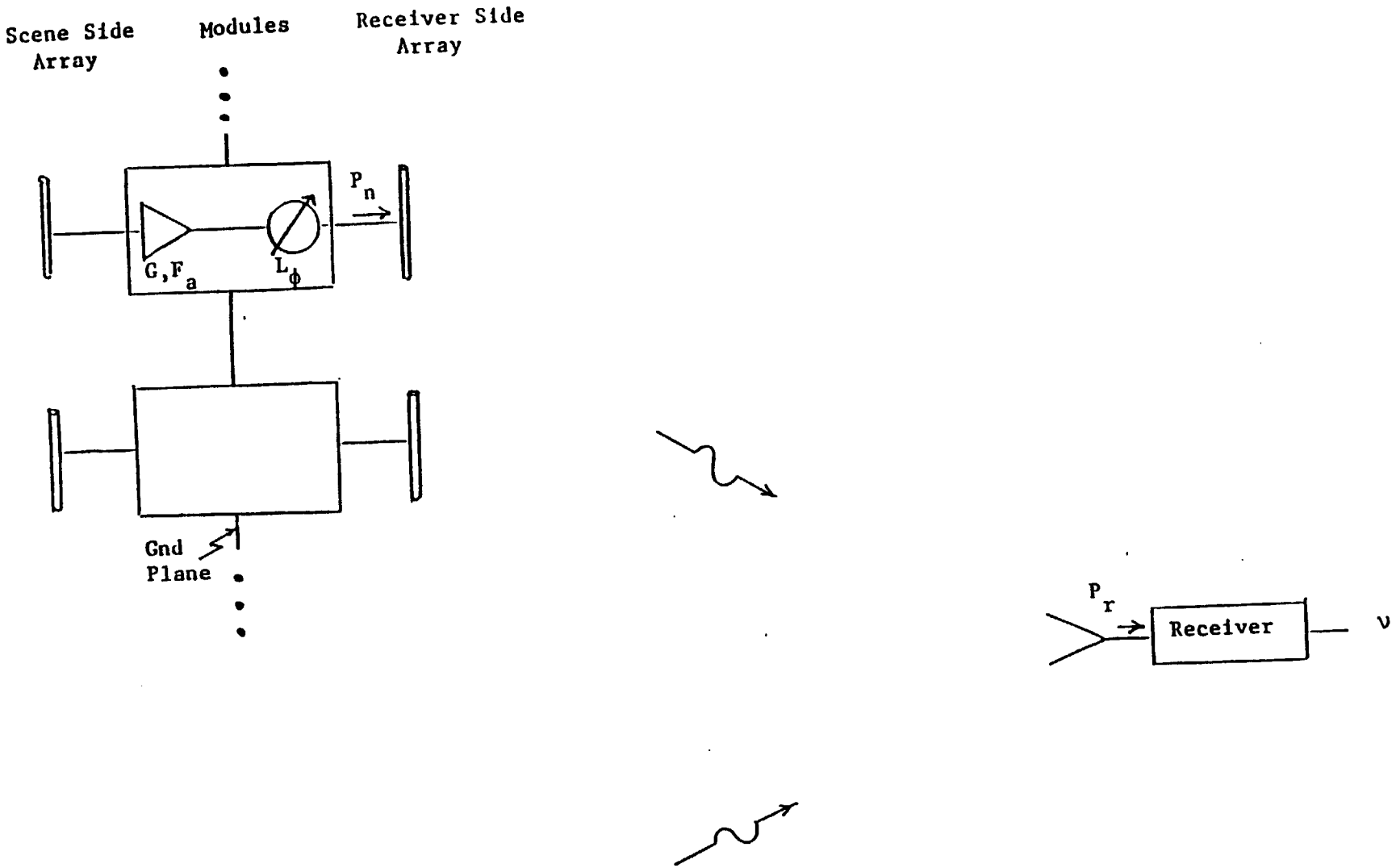

Figure 2-1. Array Lens Antenna Radiometer

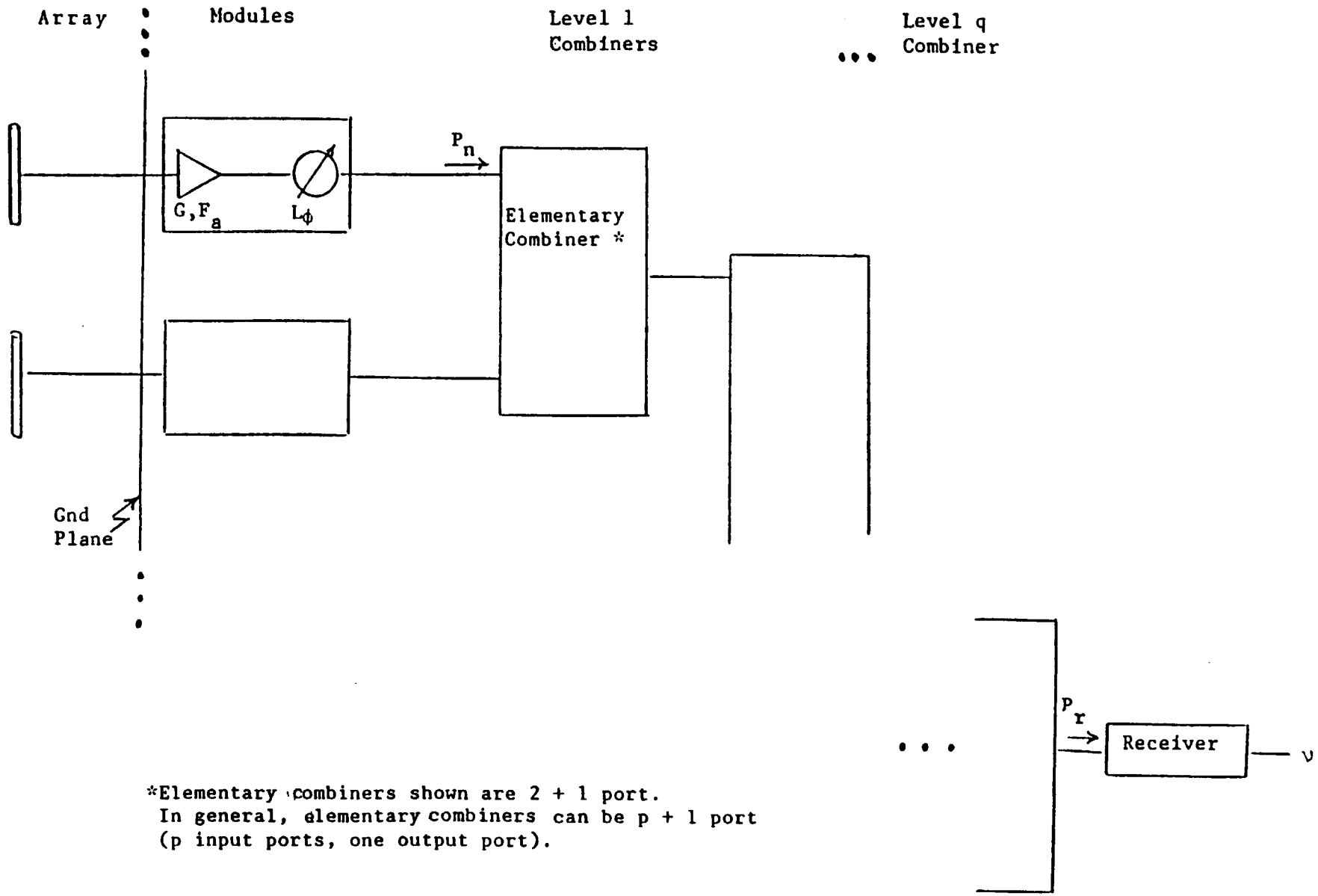

Figure 2-2. Corporate Network Array Antenna Radiometer

$$T_c = \begin{cases} f\,T_{os} & \text{Lens} \\ T_{oc}(1 - L^{-q}) & \text{Corporate network} \end{cases}$$

G = average LNA gain

L_ϕ = average phase shifter loss

G_u = average uncorrelated combiner gain

F_a = average LNA noise figure

T_o = phase shifter physical temperature

T_{oc} = corporate network physical temperature

L = average corporate network elementary combiner loss (Appendix B)

N = number of array elements (in each face array if a lens)

q = number of levels in the corporate combiner where each elementary combiner is a p + 1 port ($N = p^q$)

f = fraction of receiver antenna integrated gain corresponding to region not blocked by lens (Appendix A.4)

T_{os} = receiver antenna temperature if unblocked (typically that corresponding to deep space = 2.7 K)

The combiner uncorrelated gain is defined to be

$$G_u = \frac{P_r^u}{\bar{P}^u}$$

where

P_r^u = uncorrelated power at the receiver input port

$\bar{P}^u$ = average of uncorrelated powers available (incident) at the "combiner ports" (receiver side radiating element ports, if a lens, or first level combiner ports, if a corporate network)

The uncorrelated gain is dependent on Γ_n, F, D, and N, if a lens combiner, where

F = lens focal length

D = lens diameter

$\Gamma_n = \Gamma_n(\theta_n)$ = active reflection coefficient of n^{th} radiating element on receiver side of lens*

θ_n = angular direction from focal axis of n^{th} radiating element as viewed from receiver antenna

and is dependent on L, p, and q, if a corporate network combiner. The expressions for gain in terms of these parameters is derived in Appendix A for lens combiners and Appendix B for corporate network combiners. A receiver antenna is assumed in the lens case that optimally illuminates the lens in a sense of "maximum off boresight gain" as discussed in detail in Appendix A.

The phased array antenna generated noise temperature, therefore, is given by

$$T_{ary} = 290\,(F_a - 1)\frac{GG_u}{L_\phi} + T_o\,(1 - \frac{1}{L_\phi})\,G_u + \begin{cases} f\,T_{os} & \text{Lens} \\ T_{oc}\,(1 - L^{-q}) & \text{Corporate Network} \end{cases} \qquad (2\text{-}2)$$

where f, derived in Appendix A.4, is given by

$$f = 1 - \frac{\pi(1 - \cos^{u+1}\theta_M)}{2(u+1)\sin^2\theta_M} \qquad (2\text{-}3)$$

with

$$u = \frac{\log\,(4/\pi^2)}{\log(\cos\,\theta_M)}$$

and where θ_M is the angle subtended by the lens focal axis and the direction to the lens edge as viewed at the receiver antenna. Thus,

$$\theta_M = \tan^{-1}\,(D/(2F))$$

---

*For simplicity, it is assumed that active impedance is a function of off boresight angle and not the plane of the angle.

Noise generated by the lens combiner is assumed to arise from external noise sources residing in the portion of the receiver antenna gain pattern not intercepted by the lens. Noise generated by the corporate network combiner is assumed to arise from the insertion losses of the elementary combiner.

The uncorrelated combiner gain in (2-2) is given by

$$G_u = \sum_{n=1}^{N} g_n \tag{2-4}$$

where

$$g_n = \begin{cases} \dfrac{\gamma_n}{4\pi(F/D)^2 N} \cos^3\theta_n \left[\sin^2\left(\dfrac{\pi \sin\theta_n}{2\sin\theta_M}\right)\right]\left(1 - |\Gamma_n|^2\right)/\sin^2\theta_n & \text{Lens} \\ \left(\dfrac{1}{pL}\right)^q \gamma_n & \text{corporate network} \end{cases} \tag{2-5}$$

The γ_n factors in (2-4) represent an amplitude (power) weighting across the array aperture, perhaps achieved with variable gain LNAs. Let the powers incident on the combiner ports (receiver side radiating ports, if a lens, or first level combiner ports, if a corporate network) be given by $P_n^u = \gamma_n \, kT^u B$ where k = Boltzmann's Constant, B = predetection bandwidth, and T^u is the uncorrelated incident noise temperatures averaged over the channels and is given by

$$T^u = 290 \, (F_a - 1) \frac{G}{L_\phi} + T_o \left(1 - \frac{1}{L_\phi}\right) \tag{2-6}$$

Since

$$\bar{P}^u = \overline{\gamma_n kT^u B}$$

$$\bar{P}^u = kT^u B \, \bar{\gamma}_n$$

it is convenient to normalize the γ_n according to $\bar{\gamma}_n = 1$ or

$$\sum_n \gamma_n = N \tag{2-7}$$

If the array weighting and the combiner functions, including losses and mismatch, are axially symmetric, (2-4) becomes, from Appendix A,

$$G_u = \sum_{i=1}^{N_\rho} 2\pi(i - \tfrac{1}{2})g_i \tag{2-8}$$

where N_ρ = number of rings of uniformity. The rings are concentric with adjacent ones spaced Δ apart with Δ^2 equal to the area associated with one array element. Also, g_i is given by (2-5) with subscripts n replaced by i and the weighting factors now satisfying

$$\sum_{i=1}^{N_\rho} \gamma_i = N_\rho \tag{2-9}$$

Note that, from Appendix A, $N = \pi N_\rho$.

2.2 Signal (Correlated) Noise Temperature

Let T_A denote the antenna temperature in the absence of losses, including scan losses, and antenna amplifier (LNA) gains. If the array is combined with a reflector, the temperature T_A would be the scene induced temperature at the receiver input of a comparable sized reflector antenna that is perfectly conducting and is mechanically steerable and conventionally fed by a single antenna in place of the array.

The scene induced noise temperature at the receiver input is related to T_A, approximately, by

$$T_{sig} = G_{eff}\, T_A' \tag{2-10}$$

where

$$G_{eff} = G(G_c/N)\ (1 - |\Gamma_a|^2)\ (L_\phi L_s)^{-1} \qquad (2\text{-}11)$$

$$T_A' = \frac{1}{L_r}\ T_A \qquad (2\text{-}12)$$

$\Gamma_a = \Gamma_a(\theta_o)$ = array radiating element active reflection coefficient (scene side array, if a lens)

G_c = average correlated combiner gain

$L_r = L_r(\theta_o, \phi_o)$ = reflector/radome dissipation loss

θ_o = phased array scan angle with respect to broadside

ϕ_o = phased array scan plane

$L_s = L_s(\theta_o, \phi_o)$ = reflector illumination spillover loss

The dependence of reflector thermal loss, L_r, and spillover loss, L_s, on the phased array scan angles, θ_o, ϕ_o, is particularly relevant regarding calibration issues. The "gain" G_{eff} is the effective single port radiometric gain introduced by the scanning feed (active phased array antenna). It is not the antenna gain of the phased array antenna. Ideally, G_{eff} = G (LNA gain) but would be less than G due to insertion losses, impedance mismatch, nonperfect focussing, and scattering. G_{eff} does not include "projection loss" associated with scanned beam positions because the associated beam broadening affects resolution and not total noise temperature. The combiner correlated gain, G_c, is defined as the ratio of receiver input power due to the signal source, or scene, to the average of the signal powers P_n^c incident at the "combiner ports" (Appendices A and B). The gain is given by

$$G_c = \left(\sum_{n=1}^{N} \sqrt{g_n} \right)^2 \qquad (2\text{-}13)$$

where the g_n are given by (2-4). The incident powers are given by $P_n^c = \gamma_n k T^c B_s$ with T^c, the correlated incident noise temperatures averaged over the channels, given by

$$T^c = \left(T'_A + \left(1 - \frac{1}{L_r}\right) T_{or}\right) \frac{G}{L_\phi L_s N} \left(1 - |\Gamma_a|^2\right) \qquad (2\text{-}14)$$

where $T_{or} = T_{or}(\theta_o, \phi_o)$ is the reflector/radome physical temperature.

If the array weighting and the combiner functions are axially symmetric, (2-14) becomes

$$G_c = \left(\sum^{N_\rho} 2\pi \left(i - \frac{1}{2}\right) \sqrt{g_i} \right)^2 \qquad (2\text{-}15)$$

with N_ρ and g_i as defined in the discussion surrounding (2-8) and (2-9).

The general dependence of scene induced receiver input temperature on the phased array antenna parameters is exhibited in (2-10), wherein, for convenience, system temperatures are referred to the receiver input, a single port, rather than to the array face, even though amplifiers can reside at the array level. Beam broadening arising from projection loss (and inefficient aperture illumination for array fed reflectors) when scanning is not included in the assessment. The effect, as indicated above, would be that of reduced spatial resolution. Also sidelobe level variations with scan, of particular importance in array fed reflectors and indicative of beam efficiency variations, are not considered.

A comment, however, regarding beam efficiency is warranted. It is very difficult to achieve low diffraction pattern sidelobes in an array fed reflector antenna over any appreciable field of view (electronic steering range). Also, reflector surface inaccuracies further contribute to sidelobe energy for very large apertures. Precise aperture control for each beam position is necessary for low diffraction sidelobes. This control could be achieved only with a fully populated phased array antenna since diffraction sidelobes then can be made

arbitrarily small. The sidelobe energy of constrained fed arrays also is almost an order of magnitude less sensitive to aperture surface perturbations than is that of reflector antennas. That of array lenses is almost another order of magnitude less sensitive.

2.3 Reflector/Radome Induced Noise Temperature

The noise temperature at the receiver input arising as a consequence of reflector and/or radome dissipation losses is given by

$$T_{ref} = (1 - \frac{1}{L_r})\, T_{or}\, G_{eff} \tag{2-16}$$

2.4 Effective Noise Temperature

For a phased array antenna system, it is convenient to relate the noise temperature at the receiver input port, T, to an equivalent single port antenna noise temperature, T_{eff}. Thus

$$T_{eff} = T/G_{eff} \tag{2-17}$$

where T is given by (2-1), with T_{ary} by (2-2), and G_{eff} is given by (2-11). Thus

$$T_{eff} = T_A' + T_{e,ary} + T_{e,ref} + T_{e,rn} \tag{2-18}$$

where

$$T_{e,ary} = \frac{290(F_a-1)G_u + T_o\,(L_\phi-1)G_u G^{-1} + L_\phi T_c G^{-1}}{(G_c/N)\,(1-|\Gamma_a|^2)\,L_s^{-1}} \tag{2-19}$$

$$T_{e,ref} = (1 - L_r^{-1})\, T_{or} \tag{2-20}$$

$$T_{e,rn} = \frac{T_{rn}}{G(G_c/N)\ (1 - |\Gamma_a|^2)\ (L_\phi L_s N)^{-1}} \qquad (2\text{-}21)$$

and T_c, as indicated early in subsection 2.1, is given by

$$T_c = \begin{cases} f\ T_{os} & \text{Lens} \\ T_{oc}(1 - L^{-q}) & \text{corporate network} \end{cases}$$

SECTION 3

SENSITIVITY

Fluctuations in receiver input noise temperature, T, limit the sensitivity of a radiometer. The minimum detectable change in "scene temperature," T'_A as defined in subsection 2.2, is related to that of T via

$$\frac{\Delta T'_A}{T_{eff}} = \frac{\Delta T}{T} \qquad (3\text{-}1)$$

where "T_{eff}" and "T'_A" denote corresponding average noise temperatures. Both T and ΔT are directly related to the recorded voltage (detection stage output), ν, average and rms fluctuation values respectively.

Consider two independent contributions to the rms recorded output: noise fluctuations and amplifier instability. Assume a square law detection receiver. The recorded voltage is proportional to the receiver input temperature, and

$$\frac{\Delta T}{T} = \frac{\Delta \nu}{\bar{\nu}} \qquad (3\text{-}2)$$

where $\bar{\nu}$ and $\Delta\nu$ are the average value and rms fluctuation values of ν respectively. Let $\Delta\nu_T$ be the rms deviation of ν from $\bar{\nu}$ arising from noise fluctuations only. It can be shown that, for a square law detection/total power radiometer,

$$\frac{\Delta\nu_T}{\bar{\nu}} = \frac{1}{\sqrt{B\tau}}$$

where B = predetection bandwidth and τ = averaging time (dwell period) of the detection process.

Consider the fluctuations arising from the N amplifiers in the N element phased array antenna. Let σ_ν^2 be the variance of ν arising from amplifier

amplitude and phase fluctuations. The total rms uncertainty is given approximately by [2]

$$\frac{\Delta\nu}{\bar{\nu}} = \left(\frac{1}{B\tau} + \frac{\sigma_\nu^2}{\bar{\nu}^2} \right)^{1/2} \tag{3-3}$$

From (3-1), (3-2), and (3-3) it follows that

$$\Delta T'_A = \left(\frac{T_{eff}^2}{B\tau} + \frac{\sigma_\nu^2}{\bar{\nu}^2} T_{eff}^2 \right)^{1/2} \tag{3-4}$$

An expression relating σ_ν^2 to amplifier gain and phase fluctuations is derived in Appendix C. The essential results are discussed below. Two types of fluctuations are considered: zero mean amplitude fluctuations that are uncorrelated between amplifiers and those that are correlated between amplifiers. It is shown in Appendix C that zero mean amplifier phase fluctuations are an order of magnitude less significant than are amplitude fluctuations and thus phase fluctuations are not considered further.

It follows from the derivations in appendices A, B, and C that

$$\frac{\sigma_\nu^2}{\bar{\nu}^2} T_{eff}^2 = \frac{4\,\sigma_\alpha^2}{G_{eff}^2} \cdot \begin{cases} \sum_n g_n \left(T^u \sqrt{g_n} + T^c \sum_m \sqrt{g_m} \right)^2 & \text{uncorrelated amplifier fluctuations} \\ \left(T^u \sum_n g_n + T^c \left(\sum_n \sqrt{g_n} \right)^2 \right)^2 & \text{uniform amplifier fluctuations} \end{cases} \tag{3-5}$$

where the g_n, T^u, and T^c are as defined in Section 2, and

σ_α^2 = mean square fractional amplitude deviation of LNA voltage transfer function

In deriving (3-5), use was made of the relation

$$T = T_{rn} + T_c + T^u G_u + T^c G_c \tag{3-6}$$

where

$$G_u = \sum_n g_n \, (1 + \alpha_n)^2$$

$$G_c = \left| \sum_n \sqrt{g_n} \, (1 + \alpha_n) \, e^{j\psi_n} \right|^2$$

α_n = n^{th} LNA fractional amplitude deviation

ψ_n = n^{th} LNA phase deviation

It is readily apparent from (3-5) that if all g_n are equal, the rms variation in recorded output due to correlated amplifier fluctuations is $\sqrt{N}$ times greater than that due to uncorrelated amplifier fluctuations.

If the array weighting and the combiner functions, including losses and mismatch, are axially symmetric, (3-5) becomes

$$\frac{\alpha^2}{\nu^2} T_{eff}^2 = \frac{4 \sigma_\alpha^2}{G_{eff}^2} \cdot \begin{cases} \sum_{i=1}^{N_\rho} 2\pi \, (i-\frac{1}{2}) \, g_i \left(T^u \sqrt{g_i} + T^c \sum_{i'=1}^{N_\rho} 2\pi \, (i'-\frac{1}{2}) \sqrt{g_{i'}} \right)^2 & \text{uncorrelated amplifier fluctuations} \\ \left(T^u \sum_{i=1}^{N_\rho} 2\pi \, (i-\frac{1}{2}) \, g_i + T^c \left(\sum_{i=1}^{N_\rho} 2\pi \, (i-\frac{1}{2}) \sqrt{g_i} \right)^2 \right)^2 & \text{uniform amplifier fluctuations} \end{cases} \tag{3-7}$$

where, as before, N_ρ = number of rings of uniformity, and the g_i are as defined in the discussion surrounding (2-8) and (2-9).

SECTION 4

CALIBRATION

A means of achieving frequent calibration is highly desirable if high temperature measurement accuracy is to be realized with a total power radiometer. With amplifiers at the array level, the entire array would have to be so calibrated. Mechanical repositioning of the array to frequently point toward a calibrated source is to be avoided, if possible, because of the lengthy delay imposed. Also, it is preferable to avoid use of a rotatable flash plate since any mechanical rotation also is to be avoided if possible. Furthermore, each phased array beam position introduces different impedance match conditions which must be accounted for in the calibration.

An attractive means of calibrating all beam positions is to regularly electronically focus the array onto a controlled temperature source located off to the side of the steering volume of the array, or to the side of the subreflector in an array fed dual reflector antenna system as shown in Figure 4-1, and to combine the recorded output with tabulated data that characterizes the relative dependence of output on beam position. A study of the feasibility of this approach would be required (subsection 1.3) especially regarding tolerable variation in impedance mismatch with respect to beam position. Also, if the array is to illuminate a reflector, a change in beam position is accompanied by changes in spillover power, in concentration of power on the reflector, and in portion of the reflector illuminated. The feasibility of adjusting for these variations must be studied as well.

Thus the variation with scan of both array antenna impedance match, quantified by the transmission factor $(1 - |\Gamma_a|^2)$, and reflector illumination efficiency must be studied in assessing and developing such calibration techniques. (The reflector efficiency includes reflector surface heating loss and

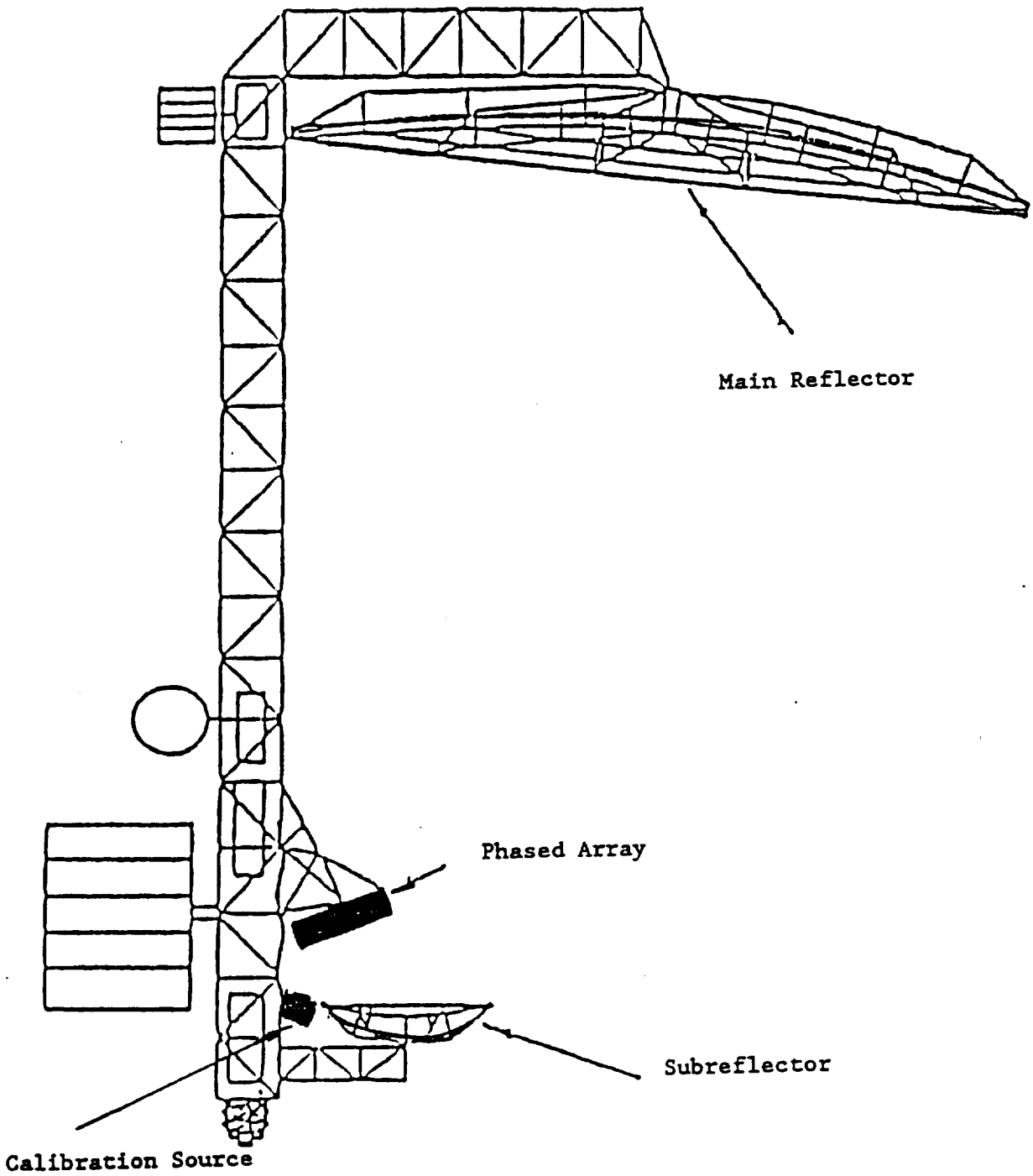

Figure 4-1. Representative Location of Controlled Temperature Source for Calibrating Phased Array

spillover loss as it relates to the array feed.) Reflected power ("double bounce" and "multiple bounce") arising from impedance mismatch within the array feed is disregarded in the modeling of Section 3 and, perhaps, can be substantially suppressed in practice by judicious use of isolators and circulators. Consideration of reflected power would entail considerably more complex modeling and would be dependent on phasing as described in Section 6-16.2 of [2]. Such modeling should be considered in an in depth analytical assessment of calibration in a candidate system.

A novel method for rapidly calibrating all beam positions of a phased array directly was recently conceived at ARC. This method would rely on polarization switching for calibration and thus is attractive only if dual polarization is not a requirement. The array normally would operate at one polarization, say horizontal, but the array elements would be switchable dual orthogonally polarized. A screen of vertically oriented wires would permanently reside in front of the array. The screen would be heated to a known, precisely monitored temperature. Upon scanning the array to a new beam position, the elements first would be switched to receive vertical polarization. A calibration measurement would be made, and the elements then would be switched back to horizontal polarization for a scene measurement. Polarization isolation would allow the scene measurement to be made without the need to move aside the screen. An investigation into the sufficiency of the isolation with respect to field of view and temperature measurement accuracy requirements would be an essential part of an assessment of the method. This method is particularly attractive if a Dicke type radiometer is required, because of the rapidity with which polarization can be switched.

SECTION 5

COMPONENTS

The more critical components of a phased array radiometer antenna are discussed here. Typical performance data is provided as well as projected performance data for solid state low noise amplifiers and phase shifters. The parameters impacting array size is presented first. Typical radiating element performance as it is affected by mutual coupling, is discussed next. LNA and phase shifter devices then are presented. This is followed with typical corporate network elementary combiner data. The section concludes with computations of corporate network combiner and lens combiner gains and corporate combiner "excess" noise temperature.

5.1 Array Size

The number of control elements (phase shifters) in a regularly spaced planar phased array increases with diameter of the array, D_a, and with the maximum scan angle ($\theta_{a,FOV}$). The relationship between an estimate of the number of control elements, N_{est}, D_a, and $\theta_{a,FOV}$ is given approximately by

$$N_{est} = .866\ \pi \left(\frac{D_a}{\lambda} \sin \theta_{a,FOV} \right)^2 \qquad (5\text{-}1)$$

where it is assumed that grating lobes are to be excluded from the scan volume (field of view) and that the lattice is equilateral triangular. Figure 5-1 contains a graph of (5-1) that demonstrates how rapidly the number of control elements increases with aperture size and field of view. If the array feeds a reflector system with aperture D, magnification Q, and maximum scan angle θ_{FOV}, then $\theta_{a,FOV}$ and D_z in (5-1) and Figure 5-1 are approximated by $\theta_{a,FOV} \approx Q\theta_{FOV}$ and $D_a \approx D/Q$.

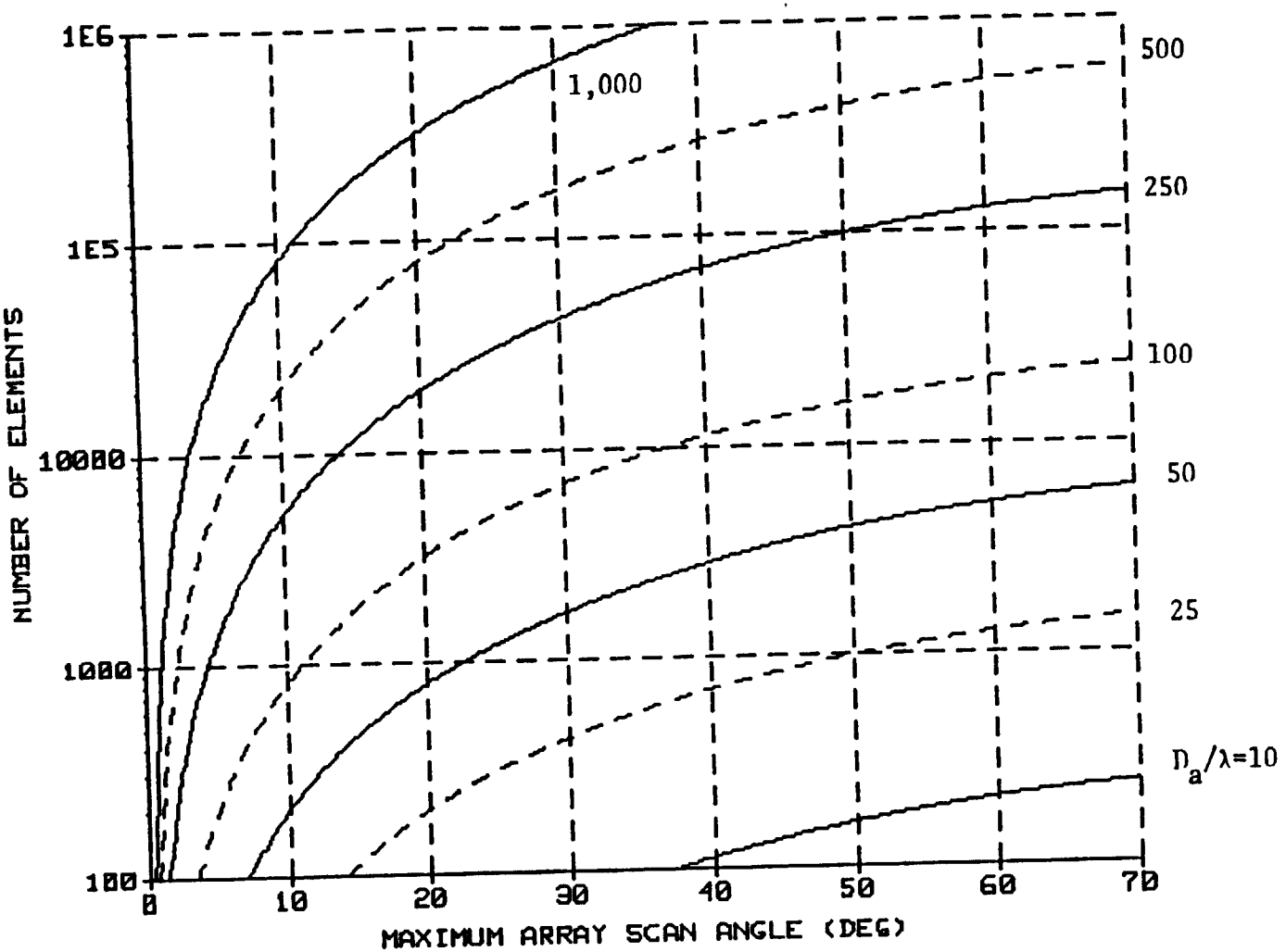

Circular Aperture
Two Dimensional Scan
Equilateral Triangular Lattice
Overlapped Subarrays

Figure 5-1. Phased Array Antenna Sizing

5.2 Radiating Elements

Radiating element performance in large planar arrays is typified by the infinite array active impedance, or, a related quantity referred to here as the transmission factor and given by

$$TF = (1 - |\Gamma|^2)$$

where Γ is the active reflection coefficient. A particularly attractive radiating element for broadband and wide field of view operation is the inclined arm folded dipole [5]. For microwave and millimeterwave systems, this element is typically composed of thin strip conductor coplanar transmission line. Figure 5-2 shows typical dimensions of the radiating element and a wide field of view lattice in terms of wavelengths corresponding to the center frequency of the effective operating band of the array. This element is particularly attractive because it can be combined with cross oriented elements to form a dual polarized element and because the inclination angle, ψ, can be selected in accordance with an optimum trade off between bandwidth and field of view. Figures 5-3 (broadside scan) and 5-4 (center frequency) demonstrate the dependence of ψ on frequency and on scan angle. Whereas the bandwidth of the arrayed element decreases with increasing ψ, the field of view increases with increasing ψ. The $\psi = 30^{o}$ inclination angle was selected as a suitable compromise between bandwidth and field of view. An approximate relationship between transmission factor; scan angle, θ; and fractional frequency deviation from center of array antenna bandwidth, β, was determined from the data in Figures 5-3 and 5-4 to be

$$(1 - |\Gamma|^2) = \cos^{4}(\theta)\ (1 - 20\ \beta^2) \qquad (5\text{-}2)$$

where

$$\beta = \frac{f - f_o}{f_o}$$

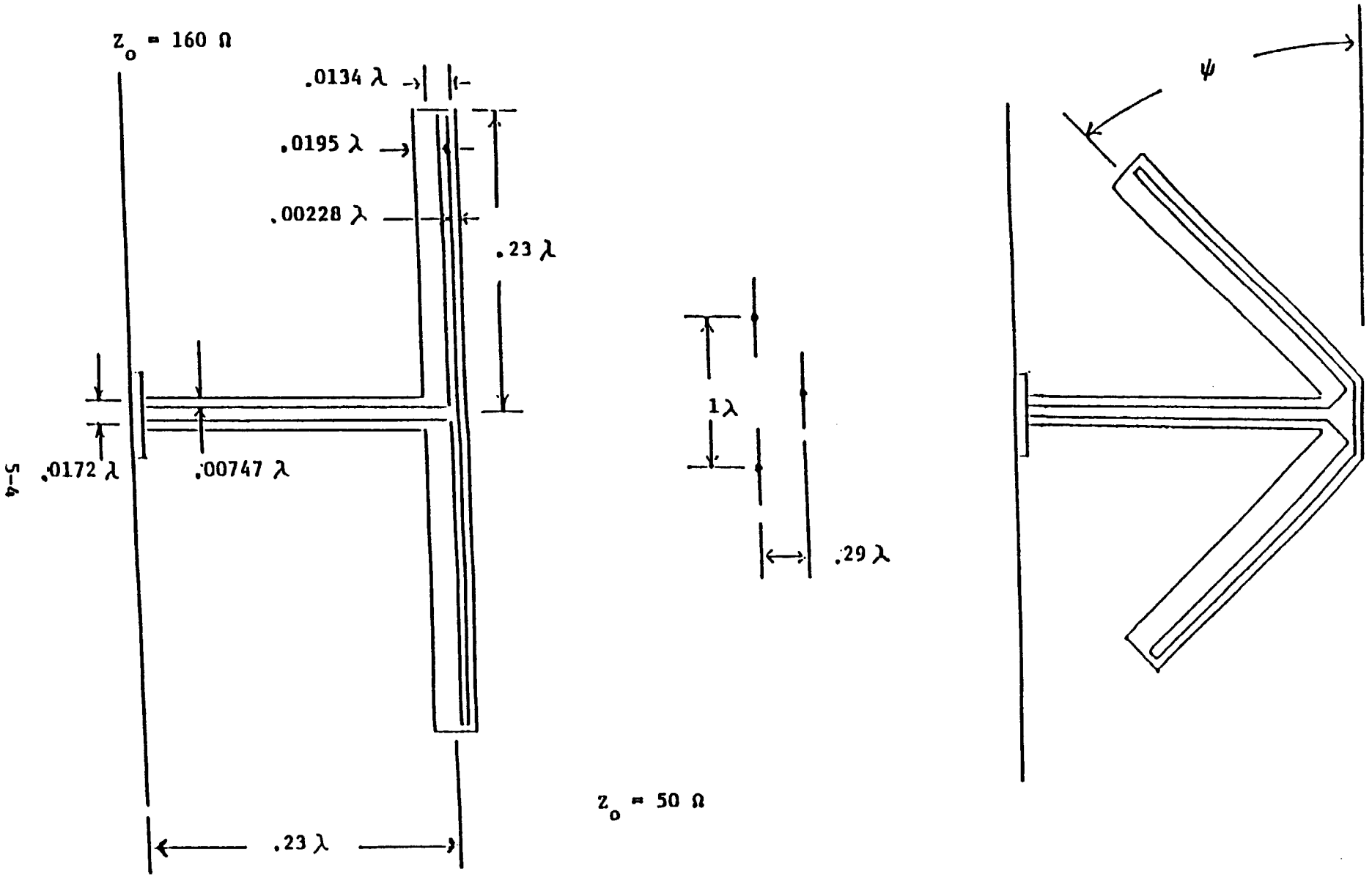

Figure 5-2. Inclined Arm Coplanar Transmission Line Folded Dipole Array

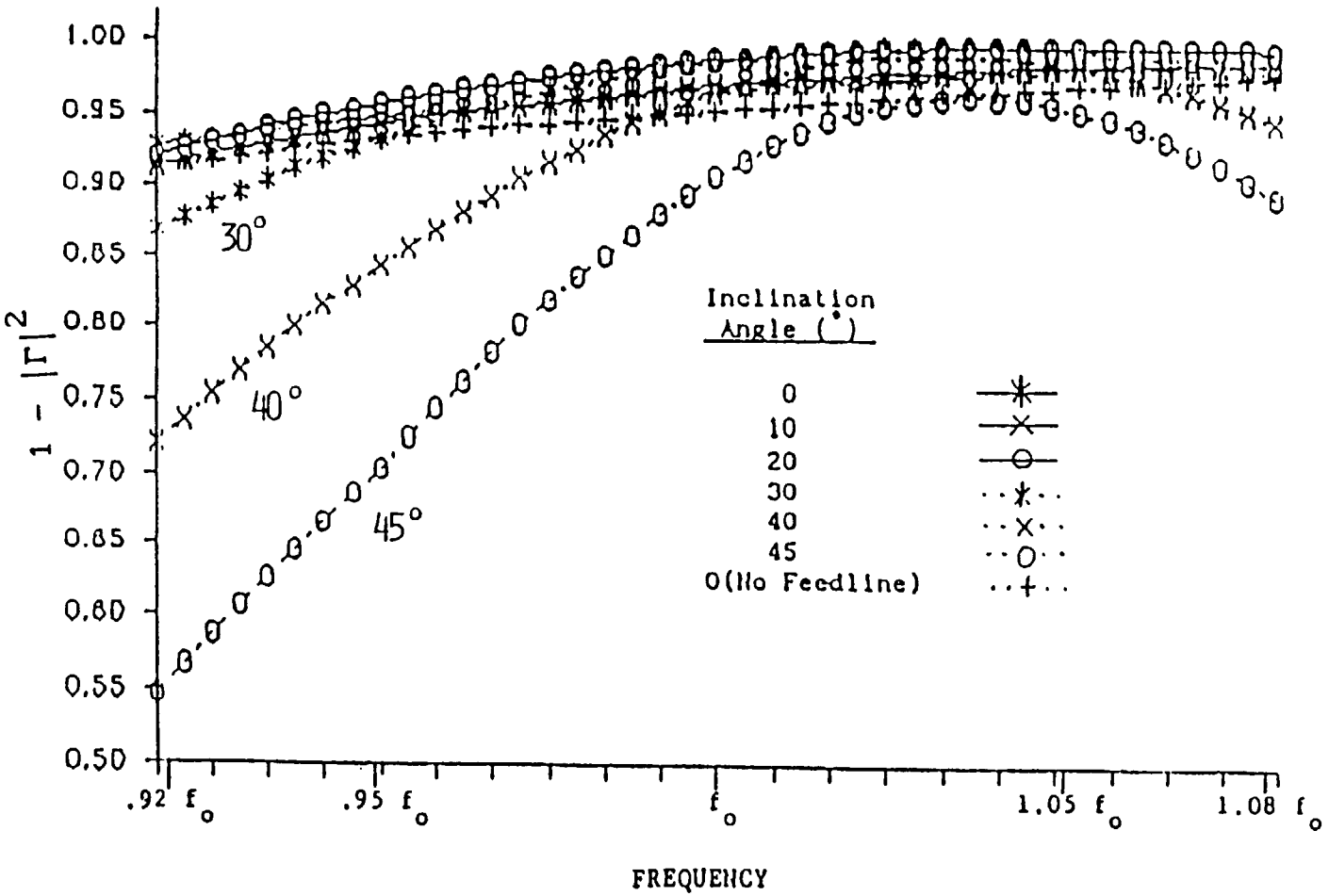

Figure 5-3. Inclined Arm Dipole Active Transmission Factor vs. Frequency at Broadside Scan

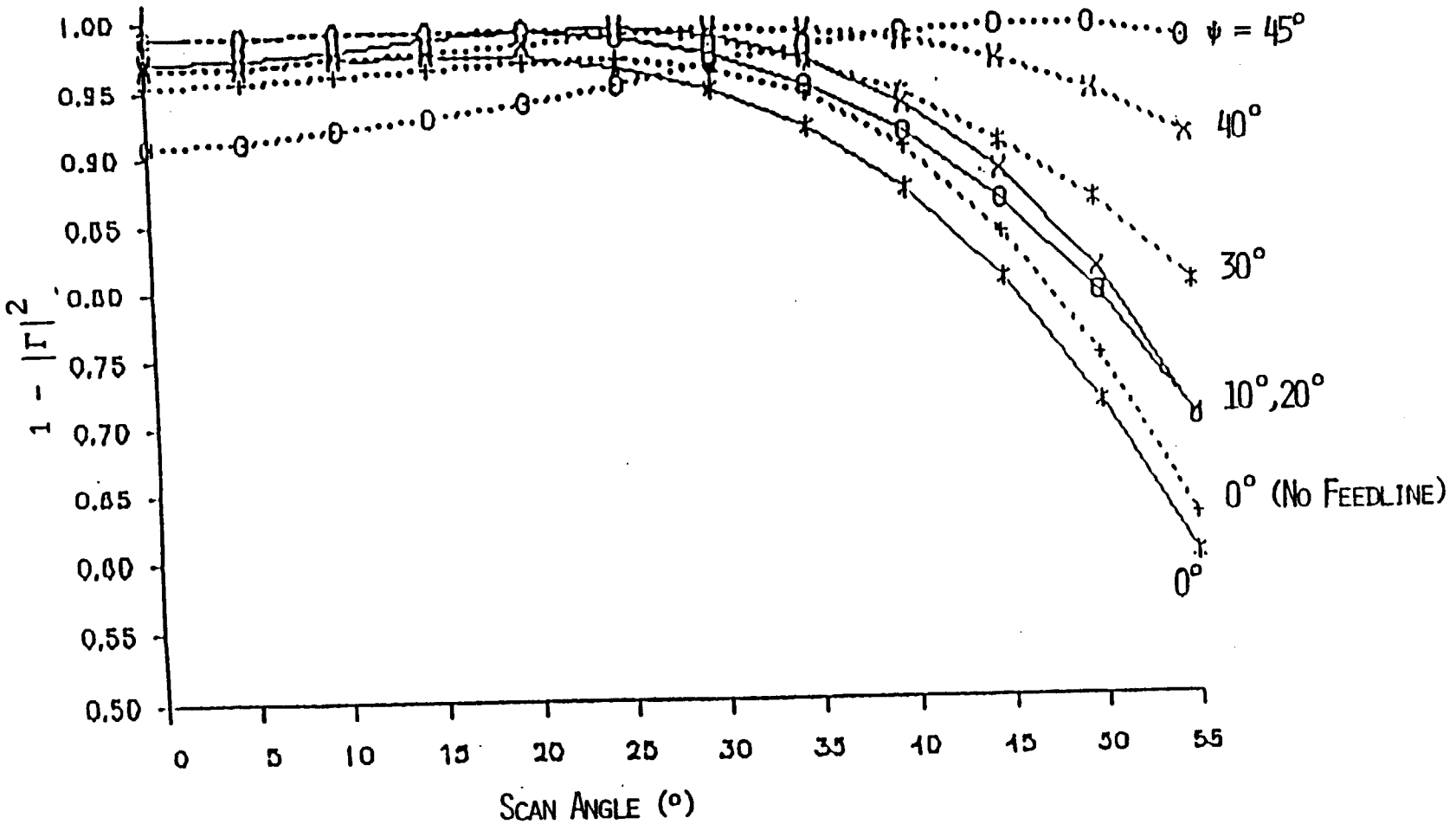

Figure 5-4. Inclined Arm Dipole Active Transmission Factor vs. E-Plane Scan Angle at Center Frequency

f = frequency

f_o = frequency corresponding to center of array antenna bandwidth

Curves generated from (5-2) are shown in Figure 5-5. A 3 dB impedance mismatch loss is evident when operating the array at the edge of an operational criteria defined by 20 percent bandwidth ($\beta = .1$) and 140^o "full" field of view ($\theta_{FOV} = 70^o$).

5.3 Devices

A comprehensive study of the present and projected state of the art solid state transmit/receive (T/R) modules was recently concluded by the Georgia Tech Research Institute for the Strategic Defense Initiative space based radar community [6]. Since the frequencies considered in that study ranged between 10 and 60 GHz, with concentration on 10 GHz and 60 GHz, the results of the study as they pertain to LNAs and phase shifters is relevant to the phased array radiometer study. The more relevant aspects of the study are summarized here.

General conclusions are grouped into "near term (1990s)" predictions and far "term" predictions. For the near term,

1. X-band (10 GHz) arrays should employ GaAs hybrid modules inserting higher level monolithic circuits as soon as practical,
2. HEMT LNA chip technology is probably mature enough for 60 GHz arrays, and
3. Ferrite phase shifter designs should be carefully scrutinized in view of significant progress in solid state technology,

and for the far term,

1. Lowest cost is perhaps ultimately achievable with single chip modules or wafer scale integration of multiple modules,

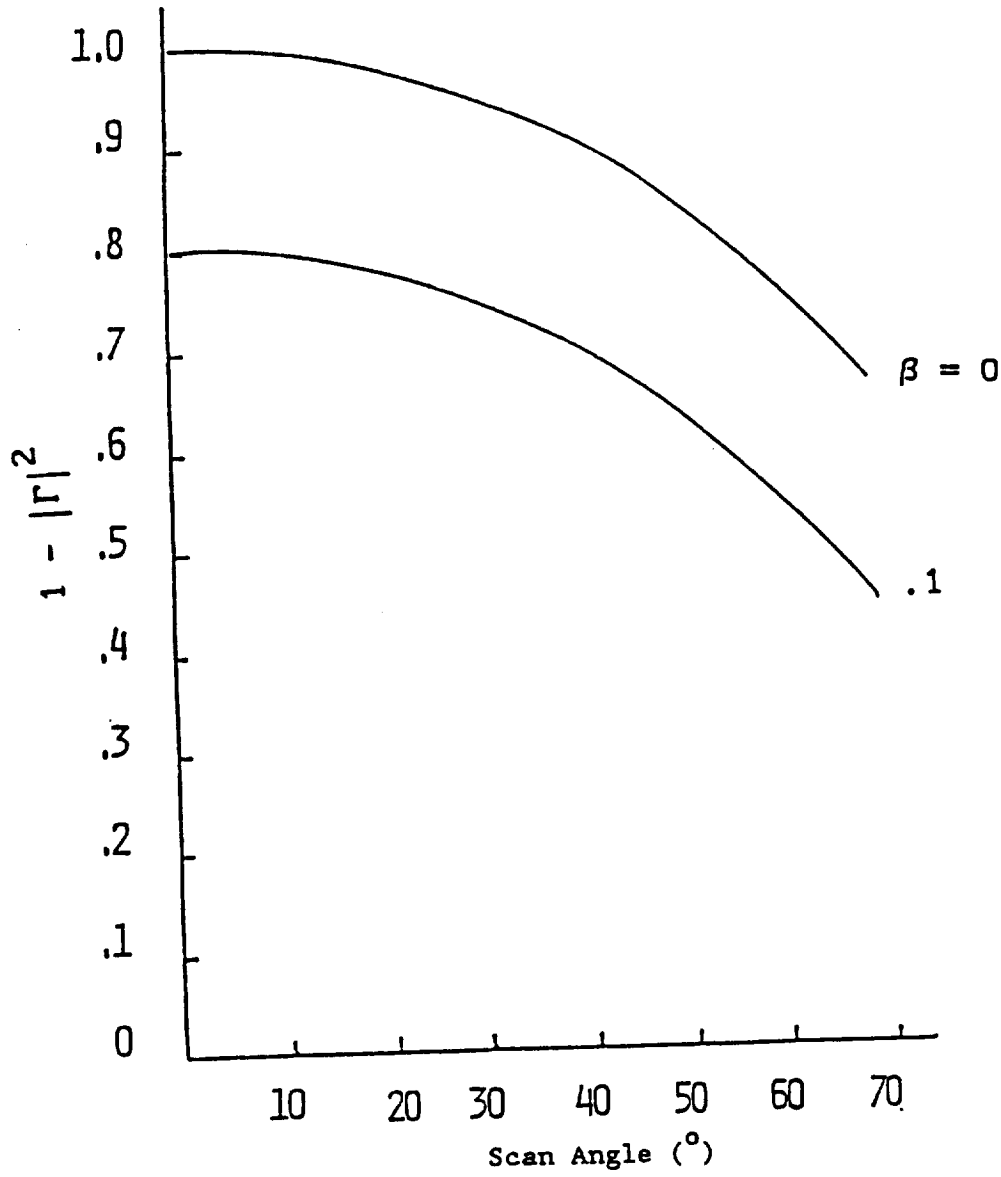

Figure 5-5. 30° Inclined Arm Folded Dipole Array Transmission Factor

2. Potentially superior semiconductor materials (e.g. INP) are not receiving significant DOD support; associated technology may soon lag that of GaAs by more than 10 years (now lags by 5 years), and
3. Machining, grinding, and polishing as used with ferrite phase shifters can never reach the high volume low cost potential of monolithic integration.

The receive mode performance of advanced X-Band T/R modules is summarized in Figure 5-6. Objectives and achievements are shown. HEMT based modules demonstrate substantial gain and correspondingly low noise figures (NF). These results are particularly noteworthy when considering that module performance includes effects of T/R switches and a ferrite circulator.

Very few T/R modules have been developed at 60 GHz. The wealth of 60 GHz data has been acquired from tests of individual devices: LNAs, phase shifters, etc. Perhaps the most noteworthy is the LNA performance achieved by GE with AlGaAs - GaAs HEMTs:

Frequency	59 - 61 GHz
NF	2.6 - 3.8 dB
Gain	6.0 - 6.8 dB
Transconductance	440 - 470 ms/mm
Total Radiation Hardness	10^7 Rads

The low noise figure is particularly noteworthy. Also, the radiation hardness is comparable to that of conventional GaAs MESFET LNAs.

Hughes researched the potential for achieving 60 GHz 5 bit digital phase shifters with 2 dB maximum insertion loss. According to [6], the "goal may not have been achieved."

Noise figures representative of a variety of device technologies are shown in Figure 5-7. HEMT is perhaps the technology of choice especially for frequencies

	Objective	Actual		
		Hybrid/	Single Chip/	Hybrid
Type	-	GaAs FETs	GaAs FETs*	GaAs HEMTs**
Avg. Gain (dB)	20	25	13.8	37
Avg. NF (dB)	4	4	5.3	2.3
Dynamic Range (dB)***	-	-	-	61.7
Manufacturer	-	Raytheon	TI	GE

* 1985 Technology. Wafer Fabrication Progressed Significantly Since 1985. This Module Type now Producible at ~$20/Module.

** 1989 Technology. Expect Similar Performance for Under $500/Module by Mid 1990s.

*** Dynamic Range Important for Low Sidelobe Weighting.

Note: Module Includes Amplifiers, Phase Shifter, T/R Switches, and Ferrite Circulator.

Figure 5-6. X-Band T/R Modules Receive Mode Performance [8]

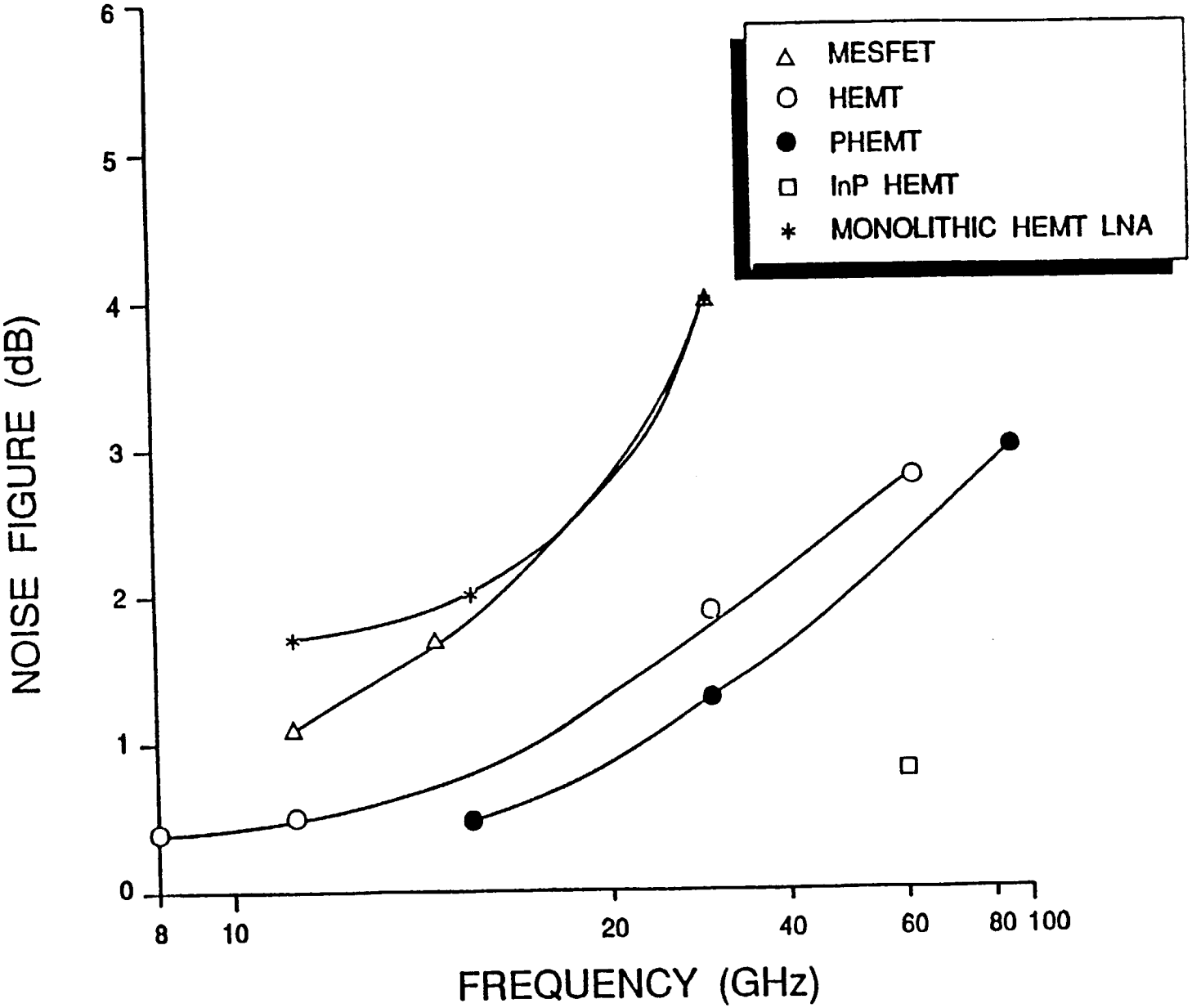

Figure 5-7. LNA Noise Figure for Various Technologies [8]

above 40 GHz. Figure 5-8 shows the gain as well as NF for a HEMT LNA. The device, although designed for 60 GHz performance, demonstrates exceptional performance at 10 GHz. Although HEMT LNA devices exhibit very low NF, the NF increases when the devices are monolithically integrated in amplifier form to achieve reasonable gain (10 to 20 dB). As shown in Figure 5-7, the NF for monolithic circuits tend to be 1 to 2 dB higher at each frequency than that for discrete devices, and the gain is typically 2 to 3 times higher. Noise figures of 4 dB or less should be achievable with HEMT based LNAs - through 60 GHz. Comparable (and less expensive) MESFET - based LNAs are feasible below 40 GHz.

One might conclude from this data that below ~ 30 GHz, and, perhaps, as high as 60 GHz, a 20 or 30 dB gain LNA/phase shifter module can be realized with overall NF under 4 dB.

5.4 Corporate Network Elementary Combiner

The corporate network combiner is assumed to be composed of a q level "tree" of p + 1 port ("p way") elementary power combiners. The dependence of number of array elements, N, on p and q is exhibited in Figure 5-9. Power combiners are characterized by high isolation between input ports, a desirable feature if the strain on calibration brought about by impedance mismatch is to be minimized.

Figure 5-10 shows the insertion loss data of several stripline combiners as abstracted from a recent Omni Spectra catalogue. The combiners were designed for 8 - 18 GHz operation. The dashed lines suggest performance at higher frequencies for similar combiner types.

5.5 Corporate and Lens Combiners

Relations for uniformly weighted lens and corporate network combiners are given in Appendices A and B, respectively. The uncorrelated combiner gain, G_u,

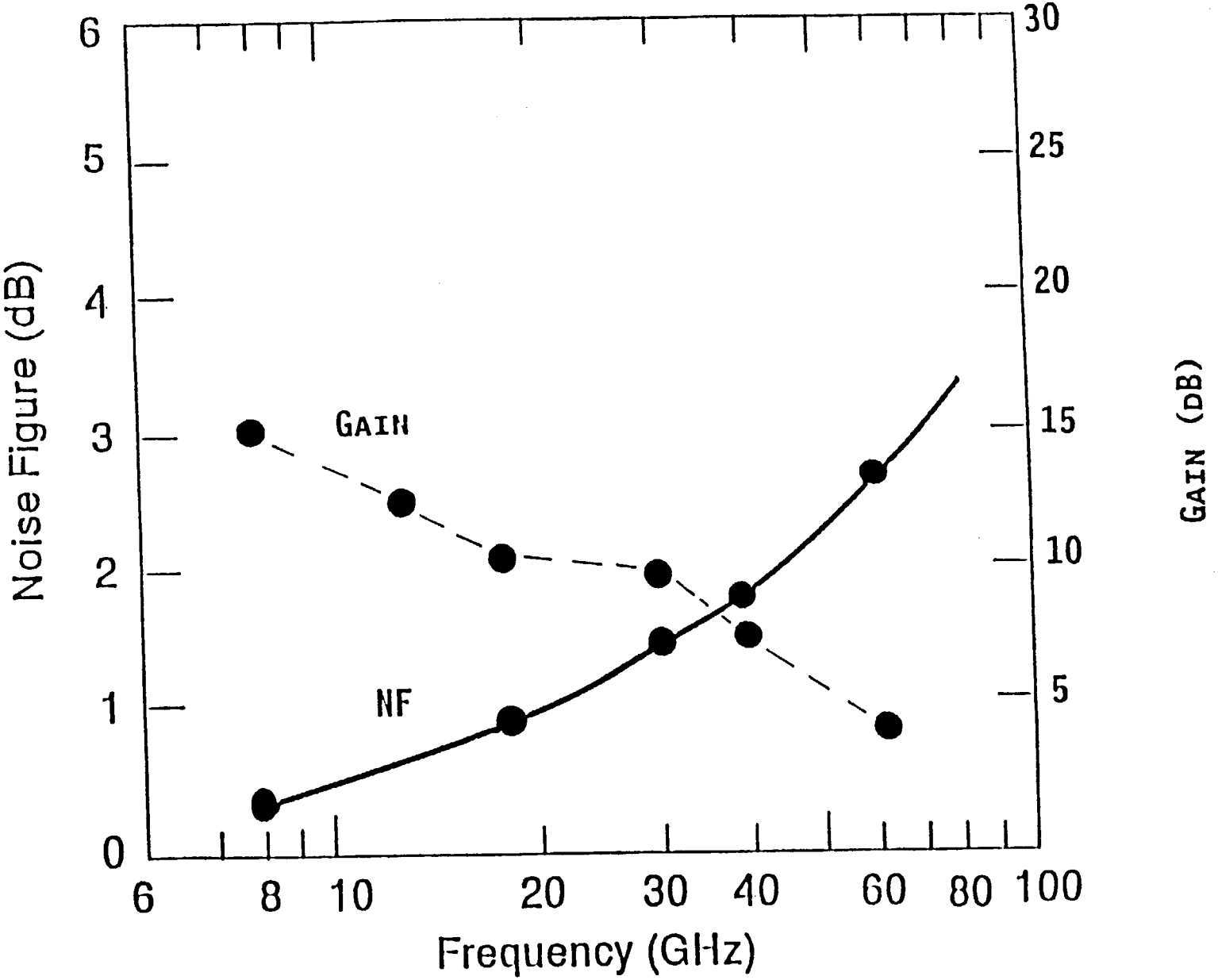

Figure 5-8. NF and Gain Frequency Dependence of a 60 GHz HEMT (GE DATA) [8]

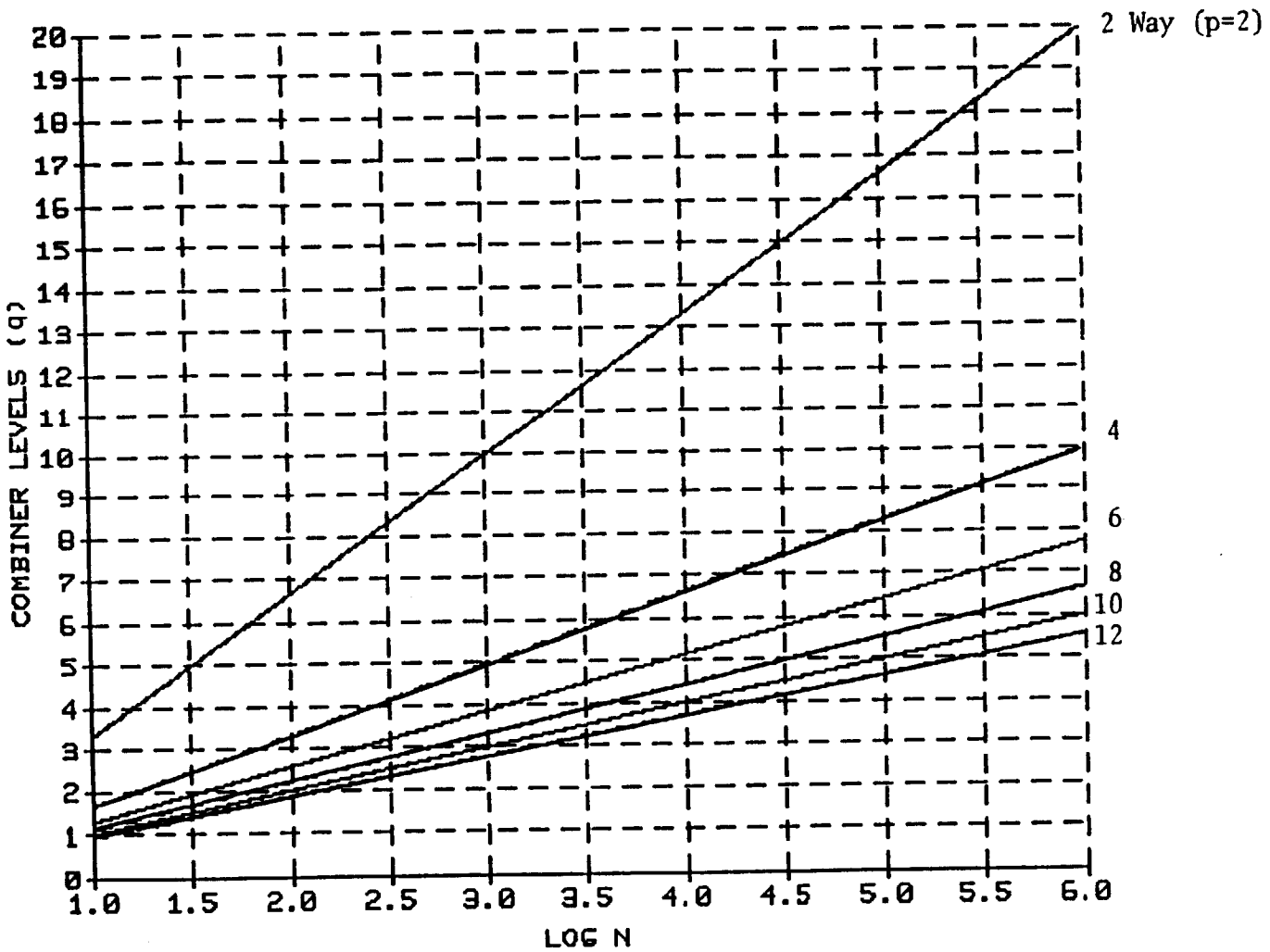

Figure 5-9. Combiner Levels vs. Array Elements

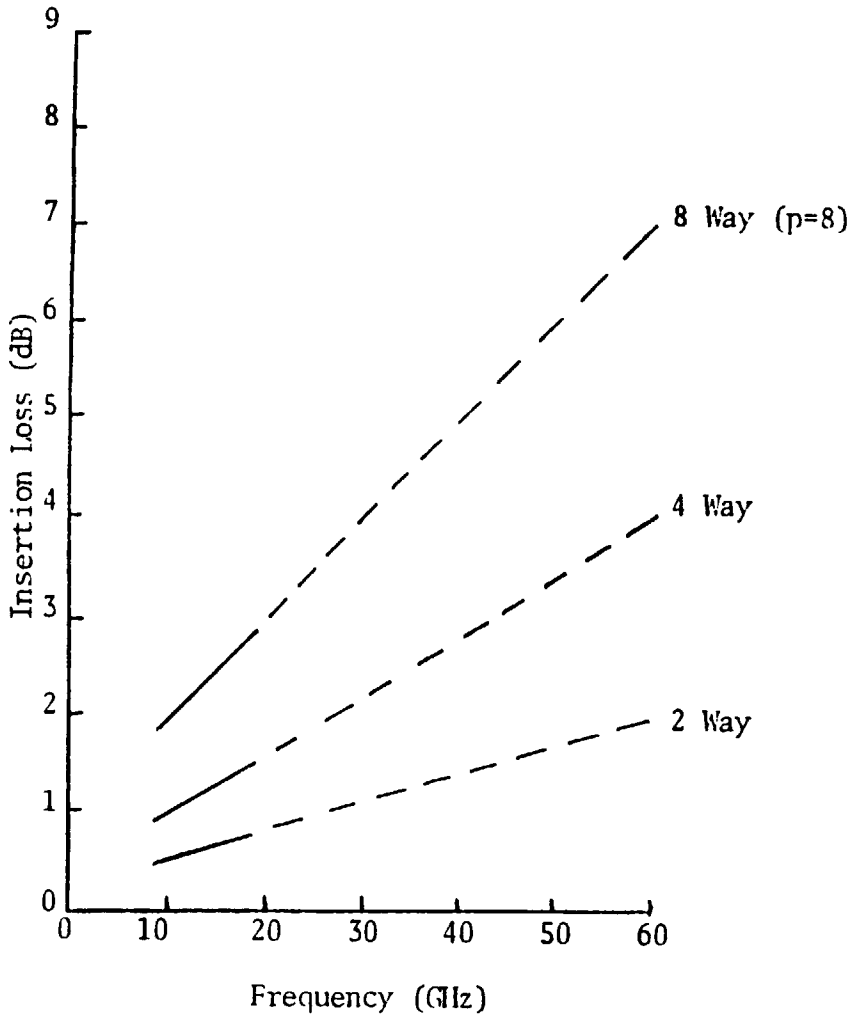

Omni Spectra
Stripline
8-18 GHz

Jan 1991

Figure 5-10. Elementary Combiner Insertion Loss

and normalized correlated combiner gain, G_c/N, for uniformly weighted corporate network combiners are plotted in Figure 5-11. $G_u = G_c/N$ for such combiners. The selected values of elementary combiner insertion loss, L, are indicative of 19 GHz components (Figure 5-10). Use of four way (p = 4) elementary combiners appears to be optimum from the stand point of maximizing combiner gain. The gains vary from ~ - 7 dB for N = 1000 array elements to ~ - 12 dB for N = 100,000 with use of four way elementary combiners. The combiner output noise temperature due to insertion loss is shown in Figure 5-12 for the same elementary combiners and for a combiner physical temperature of 200 K.

The corresponding gains for a uniformly weighted lens combiner operating at the edge of a 20 percent antenna bandwidth ($\beta = \Delta f/f_o = .1$) are shown in Figure 5-13 as functions of lens focal length to diameter ratio (F/D). The radiating element active impedance match performance indicated by the data in Figure 5-5 was assumed in computing the gains. With lens combiners, G_u and G_c/N are essentially independent of N; G_u and G_c/N differ substantially for small values of F/D; and $G_u \approx G_c/N \approx$ - 3.7 dB for F/D > .5.

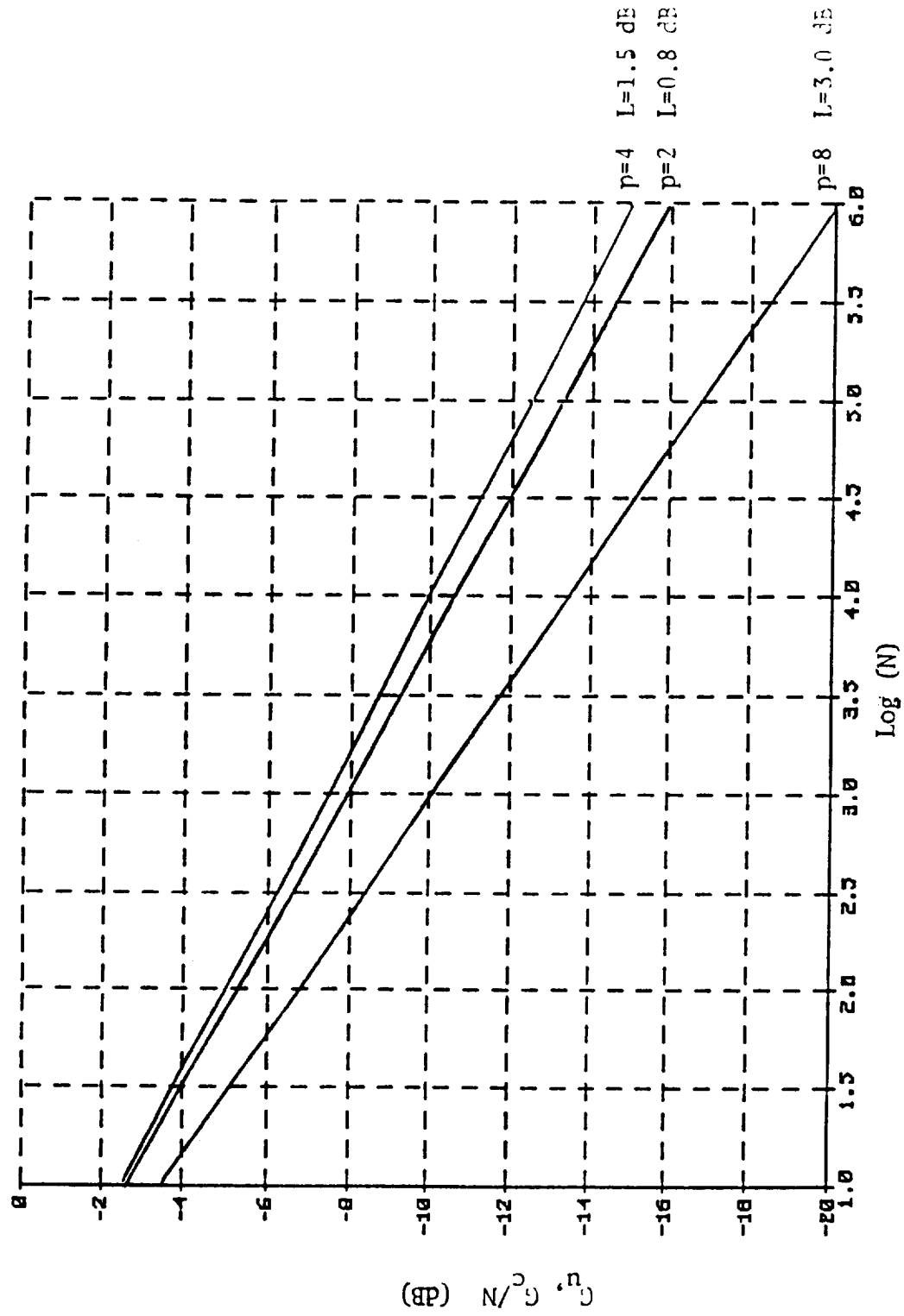

Figure 5-11. Corporate Feed Combiner Gain

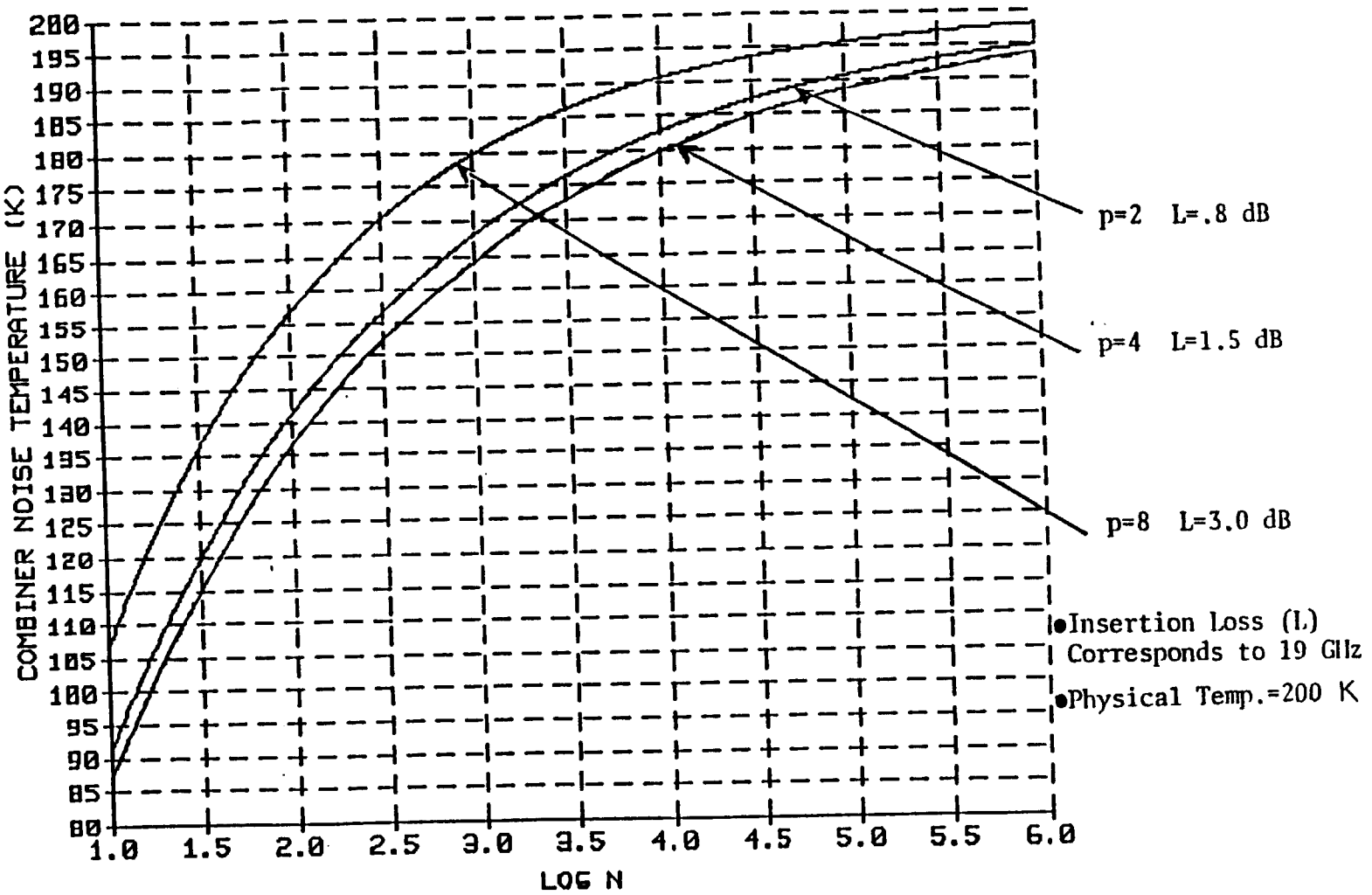

Figure 5-12. Combiner Output Noise Temperature

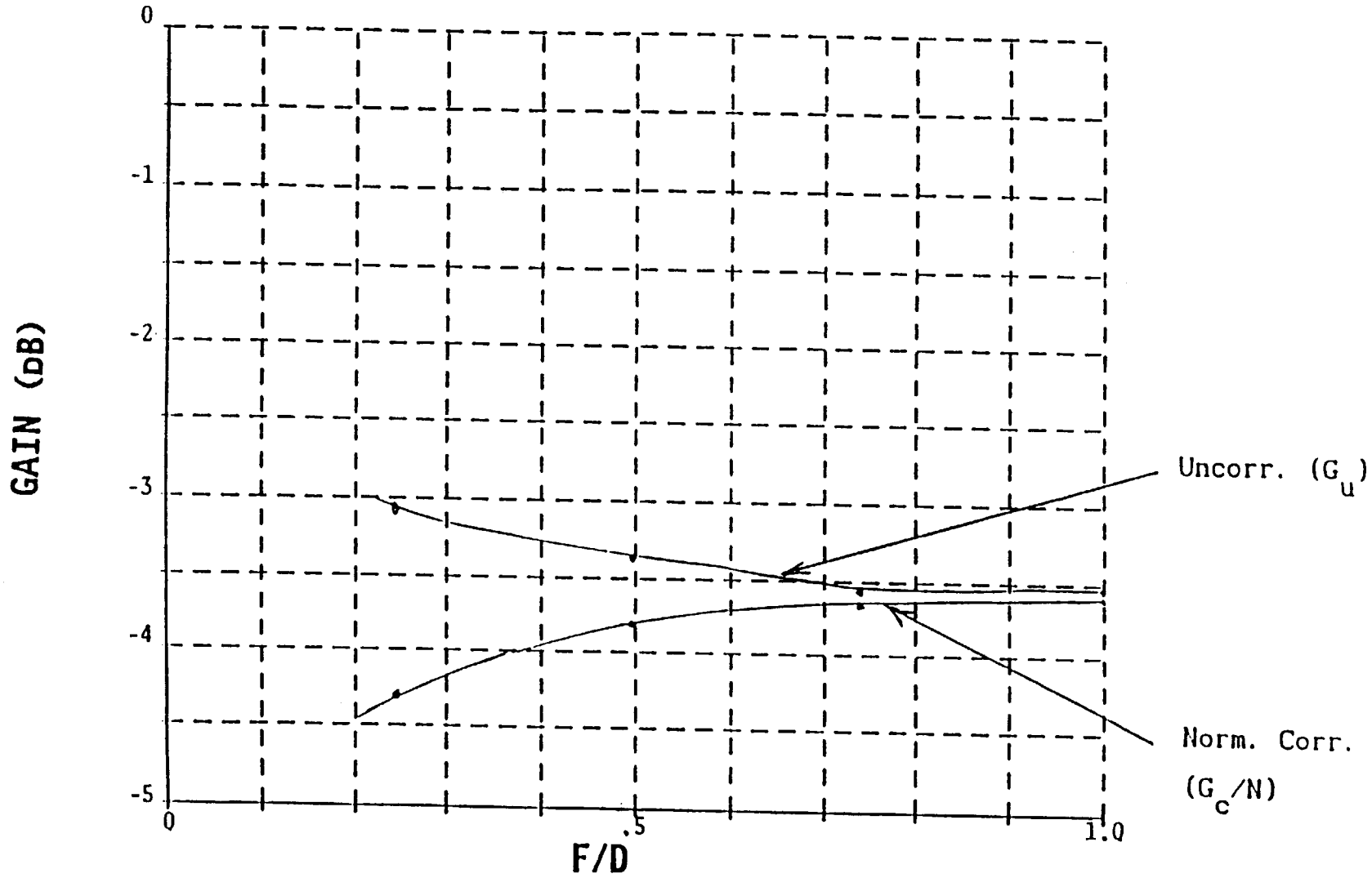

Figure 5-13. Lens Combiner Gain ($\beta = \Delta f/f_o = .1$)

SECTION 6

EXAMPLES

The modeling developed in Section 2 and Appendices A and B can be combined with the data of Section 5 to yield an estimate of that part of the system effective noise temperature contributed by the array antenna. These estimates were determined for two representative systems: a geostationary orbit array fed reflector antenna radiometer and a low earth orbit two dimensional scan array antenna radiometer.

The GEO system reflector diameter was D = 25 m and array diameter was D_a = 4 m. The maximum scan angle was $\theta_{FOV} = 7.5^\circ$ in all planes corresponding to coverage of nearly the entire earth disk. Consequently, the magnification was $Q = D/D_a$ = 6.25, the maximum scan angle of the array was $\theta_{a,FOV} = Q\theta_{FOV} = 47^\circ$, and the estimated number of array elements for 19 GHz operation was, by (5-1), N_{est} = 93,000. The "Science Benefits" study [4] concluded that a 25 m aperture reflector would yield acceptable scene temperature spatial resolution without being too large for deployment. The equatorial spot size at 19 GHz would be ~ 26 km with respect to a half power beamwidth = 1.15 λ/D (corresponds to ~ 30 dB sidelobes).

The LEO system was modeled after the DMSP Constellation Block 5D-3 (5D-2 Upgrade) as described in [4]. The orbit would be sun synchronous with 98.7° inclination, 833 km nominal altitude, and 101 min period. The current system would employ a conical scan antenna with 45° Nadir angle, 53° local incidence angle, and 1,707 km swath width. A two dimensional phased array antenna, postulated here as a replacement, would have a D_a = .5 m aperture and 1,707 km scan area diameter. The maximum scan of the array then would be $\theta_{a,FOV} = 43.7^\circ$. At 19 GHz the spatial resolution would be 31.6 km at Nadir and ~ 65 km at scan edge (range = 1,234 km), and the estimated number of elements would be N_{est} = 1,300.

The principal antenna parameters for determining the noise temperature associated with the array antenna (effective noise temperature of the array) at 19 GHz operation are given in Figure 6-1 for both systems and for corporate network as well as lens combiners for each. These noise temperatures are denoted by $T_{e,ary}$ and are defined precisely in Section 2.4.

The effective noise temperature of the array is plotted in Figure 6-2 for the GEO system. The parameters are "module" noise figure and "module" gain. (A module is assumed to contain a LNA, a phase shifter and associated circuitry. Thus, in the modeling of Section 2, F_a would now be the module noise figure, G the module gain, and L_ϕ would be set to 1.) The corporate network combiner array antenna with module gain and noise figure equal to 10 dB and 4 dB respectively would result in $T_{e,ary} \approx 1,000$ K. By increasing the LNA gains to 20 dB, the array antenna noise temperature becomes comparable to that for a lens combiner (~ 700 K). Further increase in LNA gain does not appreciably affect the array antenna noise temperature, although in an actual system further increase in gain may be required to reduce receiver generated noise. The lens combiner antenna noise temperature is independent of LNA gain because the lens combiner loss is a consequence of scattering and imperfect focussing and not insertion loss as in the case of the corporate network combiner antenna. The effective single port radiometric gains of the antennas normalized by the average LNA gain are

$$G_{eff}/G = \begin{cases} -13.6 \text{ dB} & \text{Corporate Network Combiner} \\ -5.6 \text{ dB} & \text{Lens combiner} \end{cases}$$

for the GEO example.

For large LNA gains (G > 20 dB), the noise temperature of the lens combiner is slightly higher than that for the corporate network combiner. This effect is a

SYSTEM	COMBINER	ARRAY MAX. SCAN (^{o}) $Q\theta_{FOV}$	NO. OF ELEM N	COMBINER GAIN (dB) G_c/N (NORM. CORR)	COMBINER GAIN (dB) G_u (UNCORR)	ELEM. TRANS. FACTOR (dB) $(1-\|\Gamma\|^2)$	ANT. PHY. TEMP (K) T_o, T_{oo}
GEO		47	93,000			-1.6 (β=.1, Max. Scan)	200
	Corporate			-12 (p=4, L=1.5dB) (q=8)	-12		
	Lens			-4 (F/D=.5)	-3.5		
LEO		43.7	1,300			-1.5 (β=.1, Max. Scan)	200
	Corporate			-8 (p=4, L=1.5dB) (q=5)	-8		
	Lens			-4 (F/D=.5)	-3.5		

Figure 6-1. Example Parameters

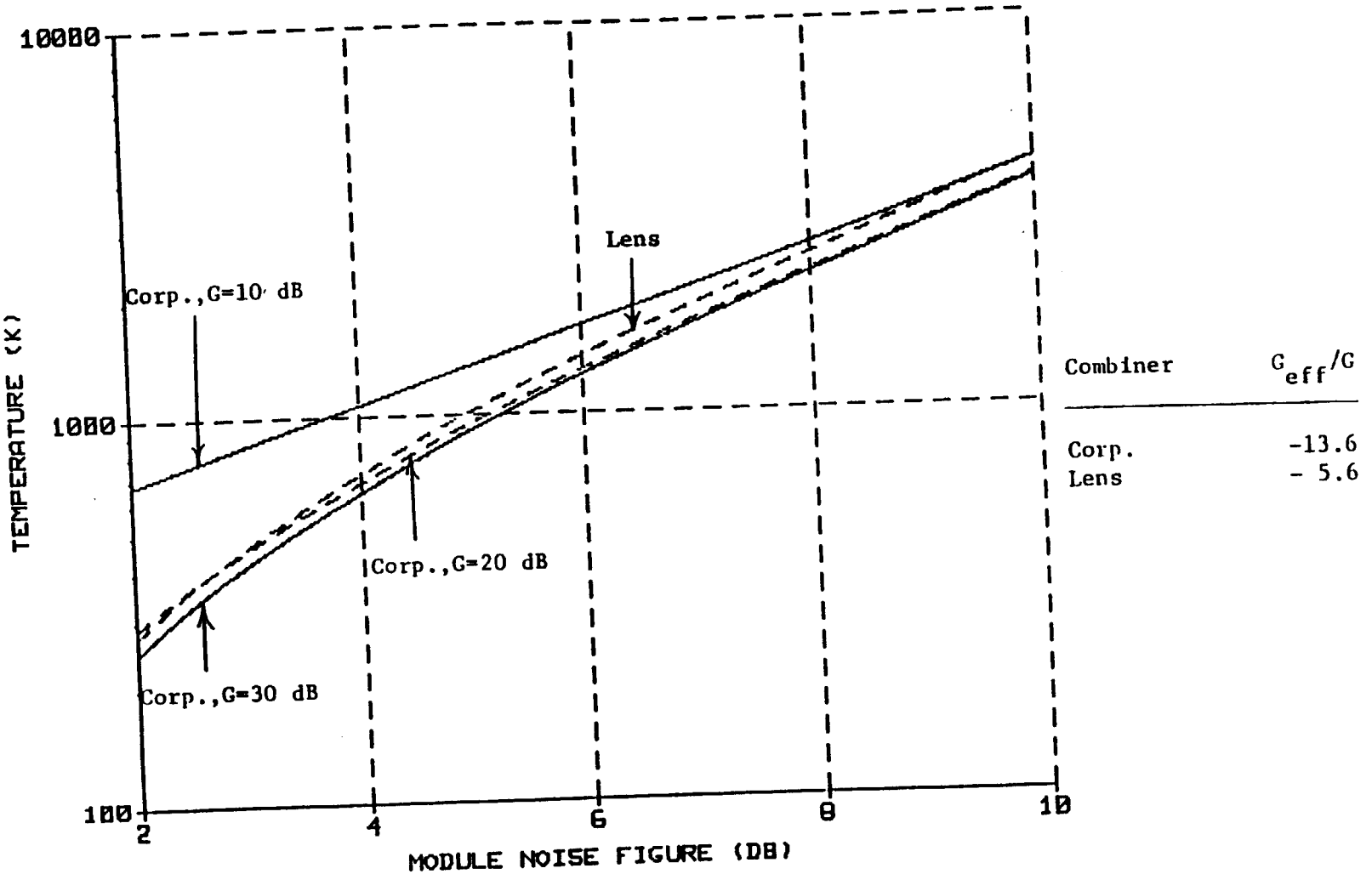

Figure 6-2. GEO System Phased Array Antenna Effective Temperature

consequence of the uncorrelated combiner gain (G_u) exceeding the normalized correlated combiner gain (G_c/N) by about .5 dB for the lens case with F/D = .5 (Figure 5-13), whereas these gains are equal in the corporate combiner case. The effect is diminished for larger F/D.

Also, the contribution to the lens combiner antenna noise temperature resulting from receiver antenna "spillover" (fT_{os} in subsection 2.1) was neglected in these computations. If the system is designed such that the part of the receiver antenna pattern not intercepting the lens array views only deep space, this contribution would be negligible. If a "hot" body is viewed, however, this contribution could be substantial.

The effective antenna noise temperature for the LEO system is given in Figure 6-3. Because the number of array elements is nearly two orders of magnitude less than for the GEO system, the corporate combiner insertion loss is substantially less, and the corresponding normalized effective gain is closer to that of the lens case:

$$G_{eff}/G = \begin{cases} -9.5 \text{ dB} & \text{Corporate Network Combiner} \\ -5.6 \text{ dB} & \text{Lens Combiner} \end{cases}$$

Consequently, the corporate combiner antenna noise temperature for the LEO system is less than that for the GEO system; temperatures $\approx$ 700 K are achievable with only 10 dB gain (NF = 4 dB) module amplifiers in the LEO case. Finally it is noted that the effective gain for the lens combiner antenna, G_{eff}, is almost independent of the number of array elements, N.

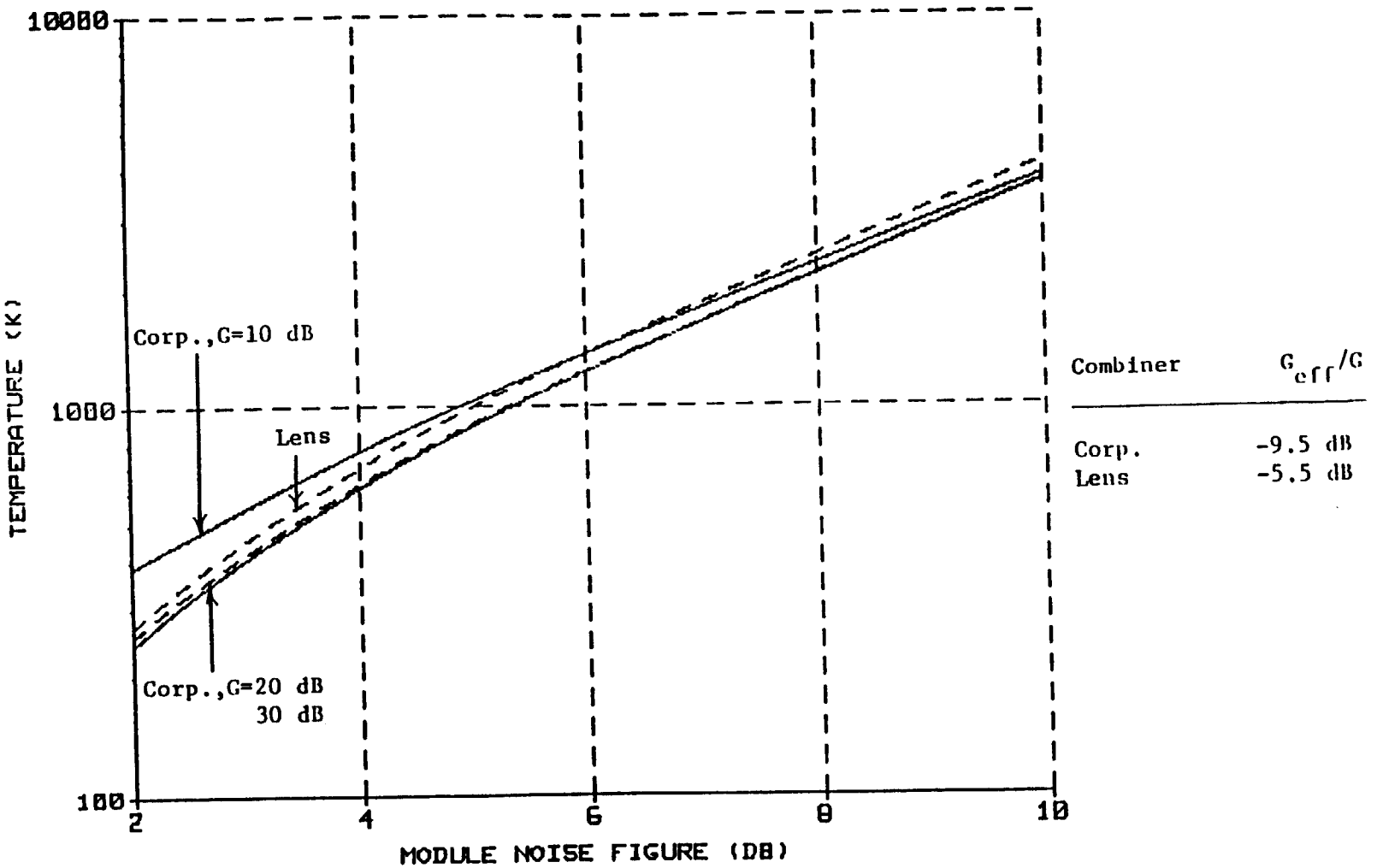

Figure 6-3. LEO System Phased Array Antenna Effective Temperature

SECTION 7

REFERENCES

1. D. Grieco, Grumman Aerospace Corporation, Space and Electronics Division, Bethpage, L.I., N.Y., Private Communication, November 1991.

2. F.T. Ulaby, et.al, Microwave Remote Sensing Active and Passive, Volume 1: Microwave Remote Sensing Fundamentals and Radiometry, pg. 368, Artech House, 1981.

3. R.R. Sahatini, ed., "The Nimbus 5 User's Guide," NASA Goddard Space Flight Center, NASA CR-139019, pg. 86, November, 1972.

4. W.L. Stutzman and G.S. Brown, eds., "The Science Benefits of and the Antenna Requirements for Microwave Remote Sensing from Geostationary Orbit," NASA Contractor Report 4408, October 1991.

5. "SDI TECHNICAL PROGRAM SUPPORT Executive Summary, System Considerations, and Antenna Technology," USAF Rome Laboratory Report RL-TR-91-126, Vol. I, June 1991.

6. "SDI TECHNICAL PROGRAM SUPPORT Module Technology and Evaluation," USAF Rome Laboratory Report RL-TR-91-126, Vol II, June 1991.

7. P.W. Hannan, "The Element-Gain Paradox for a Phased-Array Antenna," IEEE Trans. Ant. Propg., pp 423-433, July 1964.

8. T.C. Cheston, "A trilogy of Antenna Observations," IEEE Antenna and Propagation Magazine, Volume 32, pp 42-43, August 1990.

9. J.M. Howell, "Maximum Off-Boresight Gain, Revisited," IEEE Antennas and Propagation Magazine, Volume 33, pp 49-50, April 1991.

10. H.H. Grimm, "Noise Computations in Array Antenna Receiving Systems," Microwave Journal, pp 86-90, June 1963.

APPENDIX A

LENS ARRAY GAIN

Consider an array lens as shown in Figure 2-1. The power density incident on the receiver antenna due to an (available) power P_n incident on the n^{th} element feed port of the array, with all other elements terminated in the feedline impedance, is given by

$$\frac{1}{\eta} |E_n|^2 = \frac{g_n P_n}{4\pi(F/\cos\theta_n)^2} \qquad \text{(A-1)}$$

η = free space wave impedance

$E_n = E_n(\theta_n)$ = Electric intensity effective value at receiver due to n^{th} array element excitation

$g_n = g_n(\theta_n)$ = n^{th} element realized gain in the θ_n direction

θ_n = Angle subtended by line between n^{th} element and receiver and the lens focal axis

F = lens focal length

The n^{th} element realized gain is related, approximately, to the lens diameter, D, number of lens array elements, N, wavelength, λ, and infinite array active reflection coefficient, $\Gamma_n = \Gamma_n(\theta_n)$, by [7]

$$g_n = \left(\frac{\pi D}{\lambda}\right)^2 \frac{\cos\theta_n}{N} \left(1 - |\Gamma_n|^2\right) \qquad \text{(A-2)}$$

In (A-2) it is assumed that the lens lattice spacing is regular, the n^{th} element can be treated locally as if it resides in an infinite array, and the lattice is sufficiently tight to exclude grating lobes corresponding to an array scan angle of θ_n.

The available power entering the receiver, or that exiting the feed port of the receiver antenna, due to the n^{th} element excitation is given by

$$P_{rn} = \frac{\lambda^2}{4\pi} G_r \frac{1}{\eta} |E_n|^2 \qquad \text{(A-3)}$$

where $G_r = G_r(\theta_n)$ is the gain of the receiver antenna in the direction, θ_n, of the n^{th} element. From (A-1), (A-2), and (A-3), it follows that

$$P_{rn} = \frac{G_r P_n \cos^3\theta_n \ (1-|\Gamma_n|^2)}{16(F/D)^2 N} \qquad \text{(A-4)}$$

The optimum receiver antenna gain, G_r, is considered next. Expressions for G_r are combined with (A-4). The resulting expressions then are used in deriving lens gain with respect to correlated energy incident on the element feed ports and then with respect to uncorrelated energy.

A.1 Optimum Receiver Antenna Gain

The receiver antenna is assumed to have a uniformly weighted (illuminated) square aperture of side length s. Thus, the receiver antenna gain, in a principal plane, is given by

$$G_r = \frac{4 \sin^2(\frac{\pi}{\lambda} s \sin\theta)}{\pi \sin^2\theta} \qquad \text{(A-5)}$$

and (A-4) becomes

$$P_{rn} = \frac{P_n \cos^3\theta_n \sin^2(\frac{\pi}{\lambda} s \sin\theta_n)(1 - |\Gamma_n|^2)}{4\pi(F/D)^2 N \sin^2\theta_n} \qquad \text{(A-6)}$$

The correlated receiver antenna output power, P_r, assuming all lens array elements are excited with phase adjusted to focus precisely on the receiver antenna, is given by

$$P_r = \left[\sum_{n=1}^{N} \left(P_{rn} \right)^{1/2} \right]^2 \qquad \text{(A-7)}$$

where P_{rn} is given by (A-6) for principal plane angles and approximated by (A-6) for angles in other planes. An optimum length s would be one that maximizes P_r. In principal, the optimization can be executed by first approximating the summation as an integration with respect to $\theta_n \rightarrow \theta$, evaluating the integration while retaining s as a parameter, and optimizing P_r with respect to s through differentiation.

An alternative criteria with which to optimize choice of s is that which maximizes the receiver antenna gain in the direction of lens edge. This optimization has been carried out for a receiver antenna with uniformly illuminated rectangular aperture of constant width to length ratio [8]. (It has been carried out, also, for a uniformly illuminated rectangular aperture of constant width and variable length, for a uniformly illuminated circular aperture, and for an optimumly illuminated circular aperture [9].) For a square uniformly illuminated aperture of side s, the optimum s is given by

$$s = \frac{\lambda}{2 \sin \theta_M} \qquad \text{(A-8)}$$

where $\theta_M = \tan^{-1}(D/(2F))$ is the angle at the receiver antenna subtended by the lens axis and direction of lens edge. The corresponding gain, from (A-5), becomes

$$G_r = \frac{4 \sin^2\left(\frac{\pi \sin\theta}{2 \sin\theta_M}\right)}{\pi \sin^2\theta} \qquad \text{(A-9)}$$

At the lens edge, $\theta = \theta_M$, and the ratio of gain at θ_M to that at broadside is

$$\frac{G_r(\theta_M)}{G_r(0)} = \frac{4}{\pi^2}$$

or -3.92 dB, in agreement with [4], [5].

A.2 Correlated Realized Gain

The correlated receiver antenna output power, from (A-6), (A-7), and (A-8), is given by

$$P_r^c = \frac{1}{4\pi(F/D)^2 N} \left(\sum_{n=1}^{N} \left[\frac{P_n^c \cos^3\theta_n \sin^2\left(\frac{\pi \sin\theta_n}{2 \sin\theta_M}\right)(1 - |\Gamma_n|^2)}{\sin^2\theta_n} \right]^{1/2} \right)^2 \qquad \text{(A-10)}$$

where a superscript "c" is given to P_r and P_n to denote correlated power. The correlated lens array realized gain is defined here as

$$G_c = \frac{P_r^c}{\bar{P}^c} \qquad \text{(A-11)}$$

where $\bar{P}^c$ is the power of correlated signals incident on a lens array element port averaged over the number of elements, i.e.,

$$\bar{P}^c = \frac{1}{N} \sum_{n=1}^{N} P_n^c \qquad \text{(A-12)}$$

If the amplitude weighting and impedance mismatch throughout the lens are axially symmetric, the expressions for computing G_c simplify. Let Δ = element spacing along the array radial dimension, ρ, and Δ^2 the area associated with one array element. The number of elements, N_i, within a ring of width Δ centered at radius ρ_i is given approximately by

$$N_i = \frac{\pi(\rho_i + \frac{\Delta}{2})^2 - \pi(\rho_i - \frac{\Delta}{2})}{\Delta^2}$$

or

$$N_i = \frac{2\pi\rho_i}{\Delta}$$

Since

$$\rho_i = \left(i - \frac{1}{2}\right)\Delta \tag{A-13}$$

then

$$N_i = 2\,\pi\left(i - \frac{1}{2}\right) \tag{A-14}$$

and

$$N = \sum_{i=i}^{N_\rho} N_i$$

or

$$N = \pi\, N_\rho^2 \tag{A-15}$$

where N_ρ = number of rings. Since

$$N = \frac{\pi D^2}{4\Delta^2} \tag{A-16}$$

it follows from (A-5) that

$$N_\rho = \frac{D}{2\Delta} \tag{A-17}$$

a not unreasonable result if D is adjusted such that D/Δ is an even integer. The correlated power then becomes

$$P_r^c = \frac{1}{2(F/D)^2 N}\left[\sum_{i=i}^{N_\rho}\left(i - \frac{1}{2}\right)\left(P_i^c \cos^3\theta_i \sin^2\left(\frac{\pi \sin\theta_i}{2 \sin\theta_M}\right)\left(1 - |\Gamma_i|^2\right)/\sin^2\theta_i\right)^{1/2}\right]^2 \tag{A-18}$$

where the terms in (A-10) containing an element index, n, have been reordered according to a row index, i. Also,

$$\theta_i = \tan^{-1}(\rho_i/F)$$

$$\theta_i = \tan^{-1}\left[(i - \tfrac{1}{2})\Delta/F\right] \qquad \text{(A-19)}$$

Equation (A-18) was derived assuming a square lattice. Assuming, instead, an equilateral triangular lattice of triangle height Δ, the same grating lobe exclusion criteria is satisfied with 13 percent fewer elements. In that case, (A-15) remains valid and (A-16) becomes

$$N = \frac{\pi D^2}{4\Delta^2}\left(\frac{1}{1.155}\right) \qquad \text{(A-20)}$$

Thus

$$N_\rho = .93\,\frac{D}{2\Delta} \qquad \text{(A-21)}$$

With (A-21) replacing (A-17), (A-18) applies to equilateral triangular lattice arrays where Δ is the height of the triangle and the ρ_i coordinate is parallel to the height.

Lens amplitude fractional fluctuations α_n and phase fluctuations ψ_n are accounted for in (A-10) by multiplying each square root term in the summation by $(1 + \alpha_n)e^{j\psi_n}$ and, in (A-18), by $(1 + \alpha_i)e^{j\psi_i}$, where α_i and ψ_i are associated with the i^{th} ring; and computing the absolute value of the respective summations prior to squaring.

A.3 Uncorrelated Realized Gain

The uncorrelated receiver antenna output power is given by

$$P_r^u = \sum_{n=1}^{N} P_{rn}^u \qquad \text{(A-22)}$$

where P_{rn}^u, the available power exiting the feed port of the receiver antenna arising from the n^{th} lens element excitation, is given by (A-6) as in the

correlated case. It is interesting to note that by virtue of the relation (A-2) for element realized gain, the active reflection coefficient (measure of mismatch loss under the fully exited, cohered array state) is evidenced in the expressions for the uncorrelated case.

From (A-6), (A-8), and (A-22), P_r^u is given by

$$P_r^u = \frac{1}{4\pi(F/D)^2 N} \sum_{n=1}^{N} P_n^u \cos^3\theta_n \sin^2\left(\frac{\pi \sin\theta_n}{2 \sin\theta_M}\right)(1 - |\Gamma_n|^2)/\sin^2\theta_n \qquad \text{(A-23)}$$

where $P_n^u = P_n$ for uncorrelated power exciting the receiver side lens array elements. The uncorrelated lens array realized gain is defined as

$$G_u = \frac{P_r^u}{\bar{P}^u} \qquad \text{(A-24)}$$

where $\bar{P}^u$ is the uncorrelated power counterpart to $\bar{P}^c$, i.e.,

$$\bar{P}^u = \frac{1}{N} \sum_{n=1}^{N} P_n^u \qquad \text{(A-25)}$$

For the axially symmetric case,

$$P_r^u = \frac{1}{2(F/D)^2 N} \sum_{i=i}^{N_\rho} (1 - \tfrac{1}{2}) P_i^u \cos^3\theta_i \sin^2\left(\frac{\pi \sin\theta_i}{2 \sin\theta_M}\right)(1 - |\Gamma_i|^2)/\sin^2\theta_i \qquad \text{(A-26)}$$

where N_ρ is given, as before, by (A-17) for a square lattice of side Δ or (A-21) for an equilateral triangular lattice of triangle height Δ.

Fractional amplitude fluctuations α_n are accounted for in (A-23) by multiplying each P_n^u term by $(1 + \alpha_n)^2$ and, in (A-26), each P_i^u term by $(1 + \alpha_i)^2$. Phase fluctuations do not influence the uncorrelated gain.

A.4 Receiver Antenna Temperature from Lens Spillover

The contribution to receiver input noise arising from the receiver antenna pattern that is not intercepted by the lens can be approximated by first observing that the receiver antenna gain as given by (A-9) can be approximated throughout most of the main beam by

$$G_r(\theta) \approx G_r^a(\theta) = \frac{\pi}{\sin^2\theta_M} \cos^u(\theta)$$

where u is determined by satisfying the edge taper condition

$$G_r^a(\theta_M) = \frac{4}{\pi^2} G(0)$$

$$G_r^a(\theta_M) = \frac{4}{\pi \sin^2\theta_M}$$

Thus

$$u = \frac{\log(4/\pi^2)}{\log(\cos\theta_M)} \qquad \text{(A-27)}$$

The integral of the gain over the angular region subtended by the lens then can be approximated by

$$\int_0^{\theta_M} \int_0^{2\pi} G_r^a \sin\theta \, d\phi \, d\theta$$

$$= 2\pi \int_0^{\theta_M} \frac{\pi}{\sin^2\theta_M} \cos^u(\theta) \sin\theta \, d\theta$$

$$= \frac{2\pi^2}{(u+1)\sin^2\theta_M} (1 - \cos^{u+1}\theta_M)$$

Since

$$\int_0^{2\pi} \int_0^{\pi} G \sin\theta \, d\theta \, d\phi = 4\pi$$

the fraction of the integrated gain corresponding to the region external to the lens is approximated by

$$f = \frac{4\pi - 2\pi^2(1 - \cos^{u+1}\theta_M)/((u+1)\sin^2\theta_M)}{4\pi}$$

$$f = 1 - \frac{\pi(1 - \cos^{u+1}\theta_M)}{2(u+1)\sin^2\theta_M} \qquad \text{(A-28)}$$

Thus, by reciprocity, if the receiver antenna temperature arising from a continuum of uniform noise source is T_{os} when the antenna is unblocked, the receiver temperature arising from the same continuum when partially shaded by the lens is given by

$$T_{ss} = f \, T_{os}$$

where u is given by (A-27) and f by (A-28).

APPENDIX B

CORPORATE FEED GAIN

Consider a $N = p^q$ element array, as in Figure 2-2, where q = number of levels of impedance matched p + 1 port elementary combiners in a corporate feed structure. Assume all elementary combiners have identical losses. If the combiner network is at temperature T_o, it can be shown that the combiner output noise temperature due to combiner losses is given by [10]

$$T_c = T_o \frac{L^q - 1}{L^q}$$

where 1/L = the ratio of output to input powers for an elementary combiner (i.e., L expressed in dB is the elementary combiner insertion loss).

Noise from LNAs, phase shifters, isolators and, perhaps, switches, are uncorrelated between inputs to the combiner network. If all elementary combiners have identical losses, L., and if the uncorrelated noise power incident at the nth combiner port is P_n^u , the combiner network output power is given by

$$P_r^u = \left(\frac{1}{pL} \right)^q \sum_{n=1}^{N} P_n^u \qquad \text{(B-1)}$$

where the combiner network is assumed to be perfectly matched. The combiner uncorrelated gain is defined as

$$G_u = \frac{P_r^u}{\bar{P}^u} = \frac{1}{\bar{P}^u} \left(\frac{1}{pL} \right)^q \sum_{n=1}^{N} P_n^u \qquad \text{(B-2)}$$

where $\bar{P}^u$ is the average uncorrelated input power, given by

$$\bar{P}^u = \frac{1}{N} \sum_{n=1}^{N} P_n^u$$

Thus,

$$G_u = L^{-q} \tag{B-3}$$

Consider now correlated signals of powers P_n^c incident on the combiner ports. The combiner network output power (receiver input power) is given by

$$P_r^c = \left(\frac{1}{pL}\right)^q \left(\sum_{n=1}^{N} \sqrt{P_n^c} \right)^2 \tag{B-4}$$

The correlated gain is given by

$$G^c = \frac{P_r^c}{\overline{P}^c} \tag{B-5}$$

where

$$\overline{P}^c = \frac{1}{N} \sum_{n=1}^{N} P_n^c \tag{B-6}$$

If all P_n^c are equal,

$$G^c = N\, L^{-q} \tag{B-7}$$

To account for feed network amplitude fractional deviations α_n and phase deviations ψ_n, (B-1) (uncorrelated case) becomes

$$P_r^u = \left(\frac{1}{pL}\right)^q \sum_{n=1}^{N} P_n^u \,(1 + \alpha_n)^2 \tag{B-8}$$

and (B-4) (correlated case) becomes

$$P_r^c = \left(\frac{1}{pL} \right)^q \left| \sum_{n=1}^{N} (1 + \alpha_n) e^{j\psi_n} \sqrt{P_n^c} \right|^2 \tag{B-9}$$

Phase fluctuations do not influence the uncorrelated receiver power.

APPENDIX C

AMPLIFIER FLUCTUATIONS

Let α_n be the fractional amplitude deviation and ψ_n the phase deviation associated with the n^{th} amplifier in a N element phased array antenna, square law detector radiometer. The governing relationship between the α_n and ψ_n and the output voltage ν is given by*

$$\nu = a + \sum_n b_n (1 + \alpha_n)^2 + \left| \sum_n c_n (1 + \alpha_n) e^{j\psi_n} \right|^2 \qquad \text{(C-1)}$$

where the a_n, c_n, and b are constants dependent largely on the nature of the feed network that combines the amplifier outputs. The dependencies are derived in Appendix A for array lenses and in Appendix B for corporate network arrays. The terms in (C-1) containing a and b_n are a consequence of system generated noise and those containing c_n are a consequence of signal.

Equation (C-1) may be written

$$\nu = a + \sum_n b_n (1 + \alpha_n)^2 + \sum_n \sum_m c_n c_m (1 + \alpha_n) (1 + \alpha_m) e^{j(\psi_n - \psi_m)} \qquad \text{(C-2)}$$

Assume first that the α_n and ψ_n are independent with zero means and with variances given by σ_α^2 and σ_ψ^2 respectively. For small ψ_n, the average value of ν is given approximately by

$$\bar{\nu} \approx \nu_o + \sigma_\alpha^2 \sum_n (b_n + c_n^2) - \sigma_\psi^2 \sum_{n \neq m} \sum c_n c_m \qquad \text{(C-3)}$$

where ν_o is ν without "errors" ($\alpha_n = \psi_n = 0$) and is given by

$$\nu_o = a + \sum_n b_n + \sum_n \sum_m c_n c_m \qquad \text{(C-4)}$$

*Indices in summations are understood to range from 1 to N.

To simplify the derivation of an expression for the variance of ν, it is convenient to note that

$$\sigma_\nu^2 = \overline{(\nu-\bar{\nu})^2}$$

$$\sigma_\nu^2 = \overline{(\nu-\nu_o)^2} - (\bar{\nu} - \nu_o)^2 \qquad \text{(C-5)}$$

Thus it remains to determine $\overline{(\nu - \nu_o)^2}$. Since all α_n and ψ_n are independent and $\nu = \nu_o$ for all $\alpha_n = \psi_n = 0$,

$$\overline{(\nu - \nu_o)^2} = \sum_n \overline{(\nu_{\alpha_n} - \nu_o)^2} + \sum_n \overline{(\nu_{\psi_n} - \nu_o)^2} \qquad \text{(C-6)}$$

In (C-6), $\nu_{\alpha_n} = \nu$ under the constraints of $\alpha_m = 0$ for all $m \neq n$ and $\psi_m = 0$ for all m. Similarly, $\nu_{\psi_n} = \nu$ under the constraints of $\psi_m = 0$ for all $m \neq n$ and $\alpha_m = 0$ for all m. Now,

$$\nu_{\alpha_n} = a + \sum_{n'} b_{n'} + b_n(2\alpha_n + \alpha_n^2) + \sum_{n'}\sum_{m'} c_{n'} c_{m'} + 2c_n\alpha_n \sum_{n'} c_{n'} + c_n^2 \alpha_n^2$$

and

$$\nu_{\alpha n} - \nu_o = 2\left(b_n + c_n \sum_{n'} c_{n'}\right) \alpha_n + (b_n + c_n^2)\alpha_n^2$$

Thus

$$\overline{(\nu_{\alpha_n} - \nu_o)^2} = 4\left(b_n + c_n \sum_{n'} c_{n'}\right)^2 \sigma_\alpha^2 + \text{higher order terms} \qquad \text{(C-7)}$$

Similarly ,

$$\nu_\psi = a + \sum_n b_{n'} + \sum_{n'}\sum_{m'} c_{n'}c_{m'} + \text{terms in } \psi_n \text{ of powers of 2 and above}$$

$$\nu_{\psi_n} - \nu_o \approx 0$$

$$\overline{(\nu_{\psi_n} - \nu_o)^2} \approx 0 \qquad \text{(C-8)}$$

By virtue of (C-3) through (C-8), the variance of ν is given approximately by

$$\sigma_\nu^2 \approx 4\,\sigma_\alpha^2 \sum_n \left(b_n + c_n \sum_{n'} c_{n'} \right)^2 \qquad \text{(C-9)}$$

where only terms up to second order have been retained. In arriving at (C-9), note that the $(\bar{\nu} - \nu_o)^2$ part of (C-5) contains terms of forth order and above.

Consider now the case where all α_n are equal and all ψ_n are equal; i.e.,

$$\alpha_n = \alpha_c$$

$$\psi_n = \psi_c$$

for all n. This case is representative of highly correlated amplifier gain and phase fluctuations and is likely to occur if the physical temperature and amplifier supply voltage vary uniformly throughout the array face. Uniform phase variations impart no variation in ν. Let α_c have zero mean and variance σ_c^2, and denote ν by ν_c for the correlated case. Then

$$\nu_c = a + (1 + \alpha_c)^2 \left(\sum_n b_n + \left(\sum_n c_n \right)^2 \right)$$

with mean

$$\bar{\nu}_c = a + (1 + \sigma_c^2) \left(\sum_n b_n + \left(\sum_n c_n \right)^2 \right) \qquad \text{(C-10)}$$

and variance

$$\sigma_{\nu,c}^2 = \overline{(\nu_c - \bar{\nu}_c)^2}$$

$$\sigma^2_{\nu,c} \approx 4\sigma^2_\alpha \left(\sum_n b_n + \sum_n c_n\right)^2\Big)^2 \quad \text{(higher order terms omitted)} \qquad \text{(C-11)}$$

Suppose $b_n = b$ and $c_n = c$ for all n. From (C-9)

$$\sigma^2_\nu \approx 4\,\sigma^2_\alpha \sum_n (b + Nc^2)^2 = 4\,\sigma^2_\alpha\, N(b + Nc^2)^2$$

and from (C-11)

$$\sigma^2_{\nu,c} = 4\,\sigma^2_\alpha\,(Nb + N^2c^2)^2 = 4\,\sigma^2_\alpha N^2(b + Nc^2)^2$$

Thus

$$\frac{\sigma_\nu}{\sigma_{\nu,c}} = \sqrt{1/N}$$

Hence, the noise temperature measurement uncertainty due to uncorrelated amplifier fluctuations is reduced from that due to correlated fluctuations by the square root of the number of array elements where each element is associated with one amplifier.